On the Status and Mechanisms of Coastal Erosion in Marawila Beach, Sri Lanka

RATNAYAKAGE Sameera Maduranga Samarasekara [**corresponding author]**

Faculty of Engineering, University of Sri Jayewardenepura, Ratmalana, Sri Lanka E-mail: uomsameera@gmail.com

Jun SASAKI

Graduate School of Frontier Sciences, The University of Tokyo, Kashiwa, Japan

Takayuki SUZUKI

Faculty of Urban Innovation, Yokohama National University, Yokohama, Japan

Ravindra JAYARATNE

School of Architecture, Computing and Engineering (ACE), University of East London, London, UK

R.A.S. RANAWAKA

Chief Engineer's Office (Coastal Development), Coast Conservation & Coastal Resource Management Department, Colombo, Sri Lanka

Sakuntha D. PATHMASIRI

Chief Engineer's Office (Coastal Development), Coast Conservation & Coastal Resource Management Department, Colombo, Sri Lanka

Acknowledgements

This study was partially funded by JSPS KAKENHI Grant No. JP25303016. The authors would like to thank Research England for granting funds for Dr Ravindra Jayaratne (UEL) to take part in and carry out field work in 2019, data analysis, technical discussions and manuscript preparation under the Global Challenges Research Fund (GCRF). We would like to thank Editage (www.editage.com) for English language editing.

Author contributions

The design of the present study was originally developed by Sameera Maduranga Ratnayakage (SR) under the supervision of Jun Sasaki (JS) and revised with contributions of all the other authors. Material preparation, data collection, and analysis were performed by SR with the help of the co-authors. The first draft of the manuscript was prepared by SR with the revision by JS. All the authors made comments, which were accommodated by SR. All the authors confirmed and approved the final manuscript.

On the Status and Mechanisms of Coastal Erosion in Marawila Beach, Sri Lanka

Abstract

Coastal erosion remains a problem in many developing countries because of a limited understating of erosion mechanisms and management. Sri Lanka is one of the countries that recognized coastal erosion management as a governmental responsibility, in 1984. Nevertheless, erosion mechanisms have not yet been fully understood. We investigate the status and mechanisms of coastal erosion using empirically collected data and various techniques, such as GIS (Geographic Information System) analysis of satellite images, drone mapping, bathymetric surveys, hindcasting of wind-induced wave climate, questionnaires, and semi-structured interview surveys. We identified wave climate change, reduction of river sand supply, interruptions from previous erosion management measures, and offshore sand mining as potential causes of erosion considering sediment flux and rates of erosion. Erosion of Marawila Beach began during 2005–2010, and has been continuing ever since, due to a lack of integration in the beach and the entire sediment system. It is necessary to identify the long-term, large-scale changes in the sediment system through data collection. This study highlights the importance of an integrated coastal erosion management plan and could facilitate better coastal erosion management in Sri Lanka, as well as in other developing countries.

Keywords: Developing country, Coastline change, Wave climate change, Sand mining, Beach nourishment

1. Introduction

Coastal erosion is a severe hazard to the livelihood and properties of coastal communities and creates complex problems (Pranzini 2018; Rangel-Buitrago et al. 2018; Williams et al. 2018). In both developed and developing countries, such erosive coasts are managed by adopting hard engineering measures (Lloyd et al. 2013; Schmidt et al. 2014; Gari et al. 2015). Sometimes, erosion problems worsen in developing countries (Saengsupavanich et al. 2009; Saengsupavanich 2013; Rangel-Buitrago et al. 2018; Samarasekara et al. 2018) because of limited budgetary allocations (White et al. 2006) for continuous or regular monitoring. Limited archived data are one major barrier in developing countries (Jonah 2015; Ndour et al. 2018; Yin et al. 2019), which limits the number of research studies.

Sri Lanka is a developing country that identified coastal erosion as a major national problem in the early 80s (Perera 1990; Godage 1992). The Coastal Conservation Department (CCD) of Sri Lanka was established to implement the coast conservation law in 1984. In 2009, the CCD was renamed the Coast Conservation and Coastal Resource Management Department (CC & CRMD), widening its scope. Although the coastal erosion problem was identified a long time ago, the mechanisms of coastal erosion are not yet fully understood and have not been fully investigated; thus, the nexus of tension has increased between the government (CC & CRMD) and fishing and hotel communities (Samarasekara 2019). As an example, fishing union leaders claim that coastal erosion has continued owing to offshore sand mining for mega reclamation projects in Colombo. The CC & CRMD claims that the main cause of erosion is the continuous reduction in river sand supply from neighboring rivers.

Erosion initially occurred near the Maha River mouth in the late 80s and slowly extended toward Marawila (Samarasekara et al. 2018). In 1986, a barrage was constructed over the Maha River in the Bambukuliya area to prevent saltwater intrusion (Wickramaarachchi 2011). The sand discharge through the river mouth was reduced from 0.15 million m^3/y in 1984 to 0.05 million m^3/y in 2001 due to river sand mining (Indra Ranasinghe; R.M. Ranaweera Banda 1992). The government has strictly controlled river sand mining since 2004 (Karunaratne 2011), causing a 5-fold increase in the sand price (Kamaladasa 2008). Some of the traditional clay miners have illegally mined sand from the riparian area of river (Samarasekara et al. 2018). The water use demand from the river increased from 54 million m^3 in 2005 to 66 million m^3 in 2015, and many weirs were constructed along the river to extract water for drinking and domestic purposes (Fernando 2005).

The shore area between the Maha River and Negombo Lagoon was heavily eroded in the early 1990s; and, in response, the CC & CRMD protected the beach by introducing four detached breakwaters and beach nourishment in 1991 (Godage 1992). The area around the river mouth was slightly eroded in the early 1990s and significantly eroded after 2001 (Wickramaarachchi 2011). The impact of coastal erosion has not yet been researched from the perspectives of offshore sand mining, upstream detached breakwaters, or wave climate change because of limited (or difficult-to-access) data on the sediment system. This study aimed to elucidate the status and mechanics of coastal erosion in Marawila by empirically collecting available data and using the inter-disciplinary approach.

The time period of the analysis is from 1980 to 2019. The reduction in river sand supply was quantitatively studied from 1986 to 2004 because of the availability of data. The river discharge and extent of watershed sand mining influenced the supply of river sand from 2004 to 2019. The extraction of shoreline data from beach properties, bathymetry survey, wave hindcasting, and estimation of annual change in sediment transport were used to identify the impact of wave climate change on longshore sediment transport from 1980 to 2019 (39 years). The downstream beach (from the Maha River mouth to Marawila) has been severely eroded since 2001; the change in beach sediment volume was estimated from 2001 to 2019. Offshore sand mining started in 2013, and the impact of offshore sand mining was analyzed from 2013 to 2019. The causes of erosion are discussed separately in three time periods, namely from 1980 to 2000, from 2000 to 2010, and from 2010 to 2019, corresponding to the terms before erosion, the first decade of erosion, and second decade of erosion, respectively, in Marawila Beach (MB). Past studies showed that inhabitants had observed intensified climatic conditions, such as strong winds, after 2010 (Samarasekara et al. 2018) and that MB was severely eroded after 2010. Therefore, the time period after erosion was divided into the first and second decade of erosion for a more specific analysis.

2. Materials and Methods

2.1 Study site

MB is located 84 km north of the city of Colombo, on the west coast of Sri Lanka, directly facing the Indian Ocean. The beach is 6.5 km long, and it provides livelihoods to both fishing and tourism-dependent communities. The area has experienced erosion rates of 10–13 m/y (CC & CRMD 2006). Since 2004, the CC & CRMD has managed the erosion by constructing revetments, detached breakwaters, and submerged breakwaters groins, and implementing beach nourishment schemes. Fig. 1 (a) shows the spatial extent of MB and the Maha River. Fig. 1 (b) shows the spatial extent of the offshore sand mining areas, Negombo lagoon mouth, Kalani river mouth, and illegal sand and clay mining pits in the Maha River riparian area. Fig. 1 (c) shows the river riparian area, illegal sand and clay mining area. Area 1 (1 km^2) [see Fig. 1 (b)] was dredged to extract 0.8 million m^3 of sand for the nourishment of MB during December 2016 and February 2017 (Samarasekara et al. 2018). Area 2 (100 km^2) was dredged to extract 70 million m^3 of sand for reclamation projects in Colombo (CECB 2015).

Fig. 1. Spatial extent of (a) Maha River and Colombo City, (b) west coast, offshore sand mining areas, Colombo City, Negombo Lagoon mouth, Kalani River mouth, Maha River mouth, Bambukiliya barrage, and clay mining areas in the

Maha River riparian area and MB, (c) Maha River riparian area, excessive clay and illegal sand mining area, and (d) sediment cell and sediment flux including MB and Maha River mouth (Source: Google Earth, Data SIO, NOAA, U.S. Navy, NGA, GEBCO (Photograph was taken by CNES-Airbus/Digital Globe satellites in December 23, 2017)

2.2 Sediment balance in the study site

Fig. 1 (d) shows the sediment cell within the Maha River mouth and MB. The sediment budget of the investigated area (i.e., dashed rectangular area) in Fig. 1 (d), is estimated using sediment in from the neighboring sediment cell (Q_{In}) and from river (Q_{River}), and sediment out to the neighboring sediment cell (Q_{Out}), and the possible sediment exchange with the offshore area (Q_{Offshore}) and to the evolved tombolos between the river mouth and MB (Q_{Hold}). The investigated area was divided into a southern cell covering the protected beach and northern cell covering the unprotected beach. The sediment balance is derived from the erosion (or accretion) of MB (Q_{Erosion}). Equation (1) shows the sediment flux of erosion in MB (Q_{Erosion}).

$$Q_{\mathrm{Erosion}} = Q_{\mathrm{Out}} - Q_{\mathrm{River}} - Q_{\mathrm{In}} + Q_{\mathrm{Hold}} + Q_{\mathrm{Offshore}} \tag{1}$$

The wave climate generates a strong littoral current towards the north during the southwest monsoon (Dayananda 1992; Fittschen et al. 1992). The littoral drift from Colombo towards Negombo was estimated at 1.3 million m^3/y in 1992 (Fittschen et al. 1992) and 0.048 million m^3/y in 2009 (Samarawikrama et al. 2009). Q_{In} could be affected by the upstream shore protection, reduction of sediment supply from upstream rivers (such as the Negombo Lagoon and Kalani River), and offshore sand mining. The contractors associated with the Colombo South Port breakwater (which was constructed between 2008 and 2012) and Port City (which was reclaimed between 2015 and 2019) frequently undertake artificial beach nourishment under the supervision of the CC & CRMD to minimize the impact to longshore sediment transport and in accordance with the agreement between the contractors and the government.

The area between the Maha River mouth and MB (including the southern part of MB) is protected by detached breakwaters, and the littoral drift is interrupted by the evolution of tombolos behind the detached breakwaters. The capacity of littoral drift ($Q_{\mathrm{Out\_max}}$) could be equal to or greater than (Q_{Out}), ($Q_{\mathrm{Out\_max}} \geq Q_{\mathrm{Out}}$). $Q_{\mathrm{Out\_max}}$ and Q_{Offshore} might be increased by severe swell waves, which were recently observed during the southwest monsoon.

2.3 Collection of past data

The last bathymetry and topographic survey were done at Marawila in 2007 by the National Aquatic Resources Research and Development Agency, Sri Lanka (NARA). The error of depth in the bathymetry survey was approximately 0.15 m according to the surveyor (NARA 2007). A time series of water depths from October 23, 2010, to August 8, 2017, at Bambukuliya Barrage in the Maha River [see Fig. 1 (b)] was collected by the National Water Supply and Drainage Board. We also measured the barrage specifications at that site. Mined sediment volume, grain sizes, and water depths were collected by the CC & CRMD. Mining area 1 was surveyed (and observed) in February 2017, and the data was verified. Specifications of mining area 2 were taken from the review of environmental impact assessments (CECB 2015). Mining area 1 could increase Q_{Offshore} and provided sand to nourish MB. Mining area 2 could increase Q_{In}. Critical bed velocity (Ucr) data, relating to the transport of a particle in mined areas, were obtained from the literature (Van Rijn 2013). The unit construction costs of coastal protection measures per unit length of coastline were provided by the CC & CRMD. Table 1 summarizes the collected past data, measurement periods, and usage.

Table 1: Collected past data and their measurement (or estimated) periods, and usage

Collected data	**Measurement or estimated (only cost) periods**	**Usage**
The bathymetry and topography data of Marawila Beach	February 2007	To estimate sediment transport flux
Time series of water depth at Bambukiliya Barrage	October 2010 to August 2017	To estimate river discharge
Mining volume, average grain size of mined sand	February 2017	To identify the effect of offshore sand mining on sediment flux
Unit construction costs of coastal protection measures per unit length of coastline	February 2017	To compare coastal protection measures for considering better erosion management

The bathymetry and topography data, time series of water depth, and specifications of mining were used to estimate sediment transport flux and river discharge, and to identify the effect of offshore sand mining on sediment flux, respectively. The unit construction costs of various coastal protection measures per unit length of coastline were compared.

2.4 Extraction of shoreline data from beach properties using satellite images and aerial photos

Digital Globe satellite images from December 2, 2001; December 19, 2003; December 29, 2005; February 11, 2010; February 2, 2014; February 7, 2017; July 30, 2018; and May 8, 2019, were collected to identify the chronological change in shoreline orientation between the Maha River mouth and MB. The changes in the shoreline were presented relative to the shoreline on December 2, 2001, and then the accretion (and erosion) rates were calculated using the method proposed by Aedla, Dwarakish, and Reddy (2015) and Samarasekara et al. (2018).

Aerial photos were collected using a drone (DJI Phantom 4 Professional) to map 44 ha of the beach area in August 2017 and February 2019. Drone flights were performed using preprogrammed missions using the DJI GS PRO package. Aerial images were taken perpendicular to the earth's surface at 30 m altitude in 0.9 cm/px resolution, and an orthomosaic map was created using the Agisoft Photoscan package. As cloud-free satellite images were limited during the southwest monsoon period (May–September), the authors obtained detailed aerial images in both the monsoon and non-monsoon periods using the drone. Orthomosaic maps were treated similarly to satellite images; the shorelines were extracted using a method proposed by Aedla et al. (2015) and Samarasekara et al. (2018). Google Earth Pro was used to combine the two datasets. The processed orthomosaic maps were overlaid on a DigitalGlobe satellite image in Google Earth Pro. Although their resolutions were very different, the accuracy in location was in the range of 5 m, which is acceptable for the present purpose of delineating the shoreline.

2.5 Collection of beach properties

The beach slope was measured from topographic surveys during field visits in February 2017, August 2017, February 2018, and February 2019. Beach slope values before 2007 are assumed to be the same as those in 2007, as erosion rates were low (1–2 m/y) during that period (CC & CRMD 2006). A linear trend in a temporal change of beach slope was assumed between 2007 and 2017. The median particle size was taken as 0.6 mm, based on the CC & CRMD reports (Fernando 2009). Due to the rough sea conditions during the southwest monsoon period, the slopes of the breaking zone were not measured; thus, the beach slope measured in February was assumed to be the same throughout the year. The density of sediment was assumed to be 2650 kg/m^3.

2.6 Bathymetry survey

Bathymetry surveys were conducted along the Marawila coast using an echo sounder (Lawrence Hook 4 Fish Finder) in February 2017, 2018, and 2019. The transducer of the fish finder was attached to a kickboard that was towed by a small fishing boat along sounding lines, as shown in Fig. 2, which also shows the predetermined lines (L1, L2, and L3) used for comparison in cross-shore profiles. These predetermined lines corresponded to the sounding lines of the NARA bathymetry survey. An estimated cross-shore beach profile where beach nourishment occurred is shown along Line L2. Lines L3 and L1 were located upcoast and downcoast of the littoral drift, respectively.

Tidal corrections for the bathymetry were made using the ReefMaster package. We took moving averages (of 5 consecutive depth measurements) of the observed bathymetry data to minimize the effect of wave action. Bathymetry contours were plotted by interpolating the modified observations; then, the annual bathymetry change rates were calculated. The sounding lines differed for each year; therefore, Triangular Irregular Networks (TIN) surfaces were created to extract depths along the predetermined lines. According to the specification of the sounder and with consideration for wave fluctuations, an error of depth was estimated to be ~0.3 m while that for horizontal positioning was in the range of 2 m. The beach slope values were used in the calculations of volume and sediment transport capacities of the littoral drifts.

Fig. 2. (a) Photograph of kickboard (sonar was attached 6 cm below the downside-center of the kickboard); (b) maps showing boat cruise lines of bathymetry surveys for 2017, 2018, and 2019; 500 m predetermined lines (L1, L2, and L3) (Source: Esri, DigitalGlobe, GeoEye, Earthstar Geographics, CNES/Airbus DS, USDA, USGS, AEX, Getmapping, Aerogrid, IGN, IGP, swisstopo, and the GIS User Community)

2.7 Wave hindcasting

As the erosion along the western coast was initially recorded in the early 1980s, the wave simulation was carried out from 1980 to identify the starting time period of intensification of wave climate, which could potentially affect sediment transport. Hindcasting of waves was performed using a third-generation wave model called WAVEWATCH III (hereafter WW3) (Tolman 2009), using the National Center for

Environmental Prediction (NCEP) and the National Center for Atmospheric Research (NCAR) (Kalnay et al. 1996) reanalysis wind data to obtain the daily average wave properties at Marawila during January 1, 1980, to December 31, 2018. The bathymetry data was obtained from ETOPO1/ETOPO2 (NGDC 2006). Fig. 3 shows the bathymetry profile and land-sea mask within the simulation domain. A grid with a resolution of 0.125° was generated from a MATLAB module, named automated grid generation for WW3 (Chawla and Tolman 2007). The reanalysis wind data consisting of U wind and V wind at 10-m altitude in 2.5° resolution was obtained at 0000 h, 0600 h, 1200 h, and 1800 h (4 times per day). The time series of the daily averaged significant wave heights (Hs), peak wave frequencies *(fp),* and wave directions *(Θ)* were obtained at the nearest grid point (7.375° N, 79.750° E) at a depth of approximately 20 m (Tolman 2009). Due to the lack of observed data, the outputs were compared with wave conditions based on transformed wave data, which were collected at the Colombo Port.

Fig. 3. Graphical representation of WW3 grid input files: (a) bathymetric input, (b) land-sea mask input, (c) obstruction in x-direction, (d) obstruction in y-direction (obstructions are small islands), and (e) simulation grid near MB

When the Hs (or Tp (= $1/fp$)) of a certain day was greater than the 3rd quartile of the whisker-plot diagrams of Hs (or Tp), such a day was called a high-wave (or long-wave) day in this study. High-wave and long-wave days were counted in each year to identify the changes in wave climate. Furthermore, the authors grouped the respective Θ values (of high waves and long waves) into 10° intervals to analyze the linear trends of the occurrences of high waves (and long waves) in each Θ group.

2.8 Estimation of river discharge and watershed sand mining

The river discharge at the barrage was calculated using Equation (2), assuming that the barrage functioned as a weir (Hager 1987). Fig. 4 (a) shows a photograph of the barrage under flood conditions. Fig. 4 (b) shows a schematic diagram of the barrage.

$$q = CBh^{1.5} \tag{2}$$

$$\text{If } 0 < {}^{h}/_{L} \leq 0.1, \text{ then } C = 1.642\left({}^{h}/_{L}\right)^{2}$$

$$\text{If } 0.1 < {}^{h}/_{L} \leq 0.4, \text{ then } C = 1.552 + 0.0533\left({}^{h}/_{L}\right)$$

$$\text{If } 0.4 < {}^{h}/_{L} \leq (1.5\sim1.9), \text{ then } C = 1.444 + 0.352\left({}^{h}/_{L}\right)$$

where q is discharged over the weir, B is the width of the weir, h is the water height over the weir, L is the length of the weir, and C is a constant for the structure.

Fig. 4. (a) Barrage under overflowing conditions (photo was taken on August 8, 2018). (b) A schematic diagram of barrage

The mined area was calculated by demarcating the mining pits [see Fig. 1 (c)] on Google Earth Pro (the latest image was taken on February 4, 2017). The locations of sand/clay mining locations were verified by traveling 14 km upstream from the river mouth in August 2017. The depths of the mining pits were verified based on interviews (i.e., authors queried the depths from the inhabitants in the river riparian area).

2.9 Estimation of beach erosion and accretion

The coastline is defined as the permanent vegetation line of the beach; the shoreline is defined as the mean edge of the swash zone (wave breaking zone) (Oertel 2005). The shoreline is divided into small segments (r = *1, 2 …*) of length d (~1 m). Images from different days were denoted (t = *1, 2…)* . Fig. 5 (a) shows a schematic diagram of the shoreline on days t and $t + 1$. The coordinates of each point on the shorelines are known. Line AB is a known straight line, which is almost parallel to the coastline. AB can be mathematically represented as $AB: y = mx + C$. The perpendicular distance ($L_{i,r}$) of each point ($P_{i,r}$) from line AB was calculated using Equation (3). The shoreline accretion rate ($E_{\Delta t,r}$) (negative values of accretion rate represent erosion rates) between day $t + 1$ and day t was calculated using Equation (4). The time (month or year) is denoted by T. The accreted shore area ($A_{\Delta t,r}$) (negative values of accreted shore area represent eroded areas) was calculated using Equation (5). The accreted shore volume ($V_{\Delta t,r}$) (negative values of accreted volume represent eroded volume) was calculated using Equation (6). The coastline on December 2, 2011, was assumed to be t = 1 in the volume calculation. The landward section of the coastal zone was considered almost horizontal. The beach shape was assumed to be an embankment between points r and r + 1.

Fig. 5. (a) Schematic diagram of the coastline, shoreline, and beach area (plane view) showing the shoreline of day t and day t + 1, line AB, and lengths $L_{t,r}$, $L_{t,r+1}$, $L_{t+1,r}$, and $L_{t+1,r+1}$ (perpendicular distances to line AB from points $P_{t,r}$, $P_{t,r+1}$, $P_{t+1,r}$, and $P_{t+1,r+1}$, respectively). (b) Schematic diagram of cross-section (RR') showing beach area and beach slopes of days t and t + 1

$$L_{t,r} = \sqrt{\left(x_{t,r} - \frac{x_{t,r}+my_{t,r}-mC}{m^2+1}\right)^2 + \left(y_{t,r} - \frac{m^2 y_{t,r}+mx_{t,r}+C}{m^2+1}\right)^2} \tag{3}$$

$$E_{\Delta t,r} = \frac{L_{t+1,r}-L_{t,r}}{T_{t+1}-T_t} \tag{4}$$

$$A_{\Delta t,r} = \frac{d}{2}\left(L_{t+1,r} + L_{t+1,r+1} - L_{t,r} - L_{t,r+1}\right) \tag{5}$$

$$V_{\Delta t,r} = \frac{d}{4}\left[(L_{t+1,r}^2 - X_{t+1,r}^2)\tan\alpha_{t+1,r} + \left(L_{t+1,r+1}^2 - X_{t+1,r+1}^2\right)\tan\alpha_{t+1,r+1} - (L_{t,r}^2 - X_{t,r}^2)\tan\alpha_{t,r} - (L_{t,r+1}^2 - X_{t,r+1}^2)\tan\alpha_{t,r+1}\right] \tag{6}$$

2.10 Estimation of annual change in sediment transport

The daily average capacities of littoral drifts were estimated using empirical formulas, field observations, and simulated wave conditions. We adopted the US Army Corps of Engineers (CERC) and Kamphuis formulas, which are widely used in estimating littoral drifts (van Rijn 2003), and are as follows:

$$Q_{\text{Out\_max}} = 0.04830\, H_s^{2.5}\sin(2\alpha) \tag{7}$$

$$Q_{\text{Out\_max}} = 0.00203\, H_s^2 T_p^{1.5}(\tan\beta)^{0.75} {d_{50}}^{-0.25}(|\sin 2\alpha|)^{0.6} \tag{8}$$

where $Q_{\text{Out\_max}}$ is the alongshore sediment transport rate (m^3/s), H_s is the significant wave height at the breaking point (m), T_p is the peak wave period (s), α is the wave angle at the breaking point, $\tan\beta$ is the beach slope in the breaking zone, and d_{50} is the median grain diameter (µm).

3. Results and Discussion

3.1 Temporal change in shoreline

MB can be divided into five zones (A, B, C, D, and E) based on the current adaptive measures implemented in February 2017. Table 2 shows the implemented management measures and length of each zone.

Table 2. Implemented management measures in Zones A, B, C, D, and E

Zone	Length (m)	Implemented management measures (February 2017)
A	2,100	4 detached breakwaters, 1,700m long revetments
B	1,400	4 submerged breakwaters, 1,000m long beach nourishment,
C	1,000	2 detached breakwaters, 1,400m long beach nourishment
D	600	600m long beach nourishment
E	1,400	11 groins

Fig. 6 shows (a) spatial extent of MB, (b) shoreline accretion (and erosion) rates between January 2017 and August 2017, (c) those between August 2017 and February 2018, (d) those between January 2017 and February 2018, and (e) management initiatives taking place after February 2017. Fig 6 (c) also includes non-monsoon months (i.e. March and April). Beach accretion (and erosion) is small in Zone A as a result of introduced detached breakwaters and revetments. Out of the four submerged breakwaters in Zone B, two failed to maintain nourished sand. The construction of the submerged breakwater 500 m away from the detached breakwater could account for ineffectiveness of beach restoration between 2100–3000 m. The beach was accreted in Zone C in both the monsoon and non-monsoon season because of evolving tombolos. The beach in Zone D was accreted from January 2017 to August 2017. This accretion was an overestimated value because the beach nourishment had not occurred at the date of the satellite image (January 12, 2017). The groin field interrupted a portion of the transported sediments towards the north and restored the beach area in Zone E. The accreted beach in Zone E during the monsoon season was slightly eroded during the non-monsoon period. Table 3 shows the accreted (or eroded) beach area for each zone. Interventions in Zone A, Zone C, and Zone E successfully restored the respective beach areas. The shorelines in Zone B and Zone C were eroded after beach nourishment in December 2016–February 2017.

Fig. 6. (a) January 2017, August 2017, and February 2018 shorelines on a satellite image in December 2017 (Image was taken on December 23, 2017) (Source: Google Earth, Data SIO, NOAA, U.S. Navy, NGA, GEBCO) (Image was taken by DigitalGlobe). (b) Shoreline accretion rate from January 2017 to August 2017. (c) Shoreline accretion rate

from August 2017 to February 2018. (d) Shoreline accretion rate from January 2017 to February 2018. (e) Significant management initiatives that took place in 2018

3.2 Bathymetry and beach properties

Fig. 7 shows the nearshore bathymetries for (a) February 2017, (b) February 2018, and (c) February 2019. Fig. 8 shows the cross-shore profiles in February 2007 and 2017 along the predetermined lines of L1, L2, and L3. These cross-shore profiles show high erosion in the bathymetry profile up to 5 m water depth. Fig. 9 shows the changes in bathymetry (a) between 2017 and 2018, and (b) between 2018 and 2019.

Fig. 7. Nearshore bathymetry in February (a) 2017, (b) 2018, and (c) 2019 (Source: Esri, DigitalGlobe, GeoEye, Earthstar Geographics, CNES/Airbus DS, USDA, USGS, AEX, Getmapping, Aerogrid, IGN, IGP, swisstopo, and the GIS User Community)

Fig. 8. Cross-shore profiles of February 2017, 2018, and 2019 along line (a) L1, (b) L2, and (c) L3 (Source: Esri, DigitalGlobe, GeoEye, Earthstar Geographics, CNES/Airbus DS, USDA, USGS, AEX, Getmapping, Aerogrid, IGN, IGP, swisstopo, and the GIS User Community)

Fig. 9. Change in bathymetry from (a) 2017–2018 and (b) 2018–2019 (Source: Esri, DigitalGlobe, GeoEye, Earthstar Geographics, CNES/Airbus DS, USDA, USGS, AEX, Getmapping, Aerogrid, IGN, IGP, swisstopo, and the GIS User Community)

Accretion areas are shown in red, while erosion areas are in blue. The nearshore erosion was high during 2017, and eroded areas were slightly accreted during 2018. This could be due to the increased northward littoral drift during the southwest monsoon season (see Section 3.7). There was no river sand supply during the southwest monsoon of 2017, as the river mouth was closed by a sand bar between February 22, 2017, and September 4, 2017. Sediments flowed through an opened river mouth after September 4, 2017. The slight accretion in 2018 could be due to river sediments and off-shoreward movement of nourished sediment caused by severe wave conditions in 2017.

Fig. 10 shows the change in the average beach slope at the depth of the wave breaker zone (d_b) for each zone. The breaker zone was determined from calculated *Hs* values ($d_b = H_s/0.7 = 3.6$ m). Fig. 10 shows the average slope values (at d_b) throughout each zone. Adaptive measures were not introduced in

2007, and beach slope values were taken from Samarasekara et al. (2018). The beach slope increased with time with implementation of various adaptive measures, although some beach areas were restored by adaptive measures. The beach slope was steepened during the rough monsoon season in 2017. The beach slope decreased in Zone B, Zone C and Zone D owing to off-shoreward transport of nourished sediment in 2018. However, the beach slope did not recover in Zone A and Zone E.

Fig. 10. Change in average beach slope of braking zone in Zones A, B, C, D, and E

3.3 Watershed environment

This section describes the temporal change in Q_{River}. Even with strict regulation of river sand mining in 2004 imposed by the government of Sri Lanka, river sand flow was further reduced owing to (i) illegal sand/clay mining from the river riparian zone and (ii) increased water demand in the watershed (as a result, dams were constructed along the river). There is comprehensive legislation and policy to mitigate the river degradation (e.g., Mined and Mineral Act, 1992 and Coastal Zone Management Plan, 2004). However, the law is not effectively enforced due to various factors, such as limited resources for supervision. The government gives priority to the construction of barrages to extract drinking water. Due to all the above factors, sediment flow will further reduce in the future. The depths of the mining pits ranged from 0 to 7 m. Approximately 10.7 million m^3 (0.82 million m^3/y) of clay and sand were removed from the riparian zone during 2004–2017. Fig. 11 shows the daily average discharges over the Bambukuliya Barrage. The time series starts on October 23, 2010 and ends on August 8, 2017. The river water discharge was drastically reduced in recent years as a result of droughts upstream and increased water demand. The maximum river flow also decreased in recent years, as there were many days with zero discharge (no flow over barrage) and flash flood sediment flows decreased. Fig. 11 clearly shows that there were many zero discharge days (closed river mouth) and fewer flood events that cause flash and bulk sediment flows to the coast. Therefore, there was a drastic reduction in the river sediment supply.

Fig. 11. Daily average river flow over Bambukiliya Barrage

3.4 Offshore sand mining

The entire northward coastline up to Marawila (including Zone A) was protected by detached breakwaters, revetments, and groins. Therefore, the sediment influx (Q_{In}) has remained low and has reduced since 2004. The mined sand heights were low compared to the water depth. The critical bed velocities were higher than the maximum orbital velocities at the seabed (see Table 3). This analysis shows that offshore sand mining has little impact on Q_{In}.

Table 3. Summarized details of offshore sand mining in Area 1 and Area 2

	Mining Area 1	Mining Area 2
Mining Period	December 2016 to January 2017	October 2013 to January 2019
Mined Sand Volume (10^6 m^3)	0.8	70
Mined Area (10^6 m^2)	4	100
Sediment depth at mines (m) =(Mined sand volume)/(mined area)	0.2	0.7
Median particle size (d_{50}) (mm)	0.2	0.5
Critical bed velocity (U_{cr}) to transport sediment (ms^{-1})	0.42	0.38
Water depth (m)	12	16-18
Maximum orbital velocity of seabed (U_b)of nearshore boundary of the mining area (ms^{-1})	0.28 (<0.42)	0.18 (<0.38)

The critical bed velocity (Ucr) to transport a particle of 0.5-mm grain size is 0.42 $m{\cdot}s^{-1}$. The area was 12 m deep and flat, and two 15 m deep pits were found during the observation, which was the maximum depth allowed by the CC & CRMD. The maximum orbital velocities at seabed (U_b) of the shoreward boundary are in the vicinity of 0.28 $m{\cdot}s^{-1}$. The (U_b) values were calculated for high-waves and the maximum value has been documented. The critical bed velocities are ~0.38 $m{\cdot}s^{-1}$. The orbital velocities at seabed (U_b) of the shoreward boundary are ~0.18 $m{\cdot}s^{-1}$.

3.5 Wave hindcasting

Previous research on the wave climate of Sri Lanka considered four seasons namely, inter-monsoon I (March–April) southwest monsoon (May–September), inter-monsoon II (October–November) and northeast monsoon (December–February) (Gunaratna, Ranasinghe and Sugandika 2011; Thevasiyani and Perera, 2014; Bamunawala et al., 2015); the simulated climate data was plotted separately for each season. Fig. 12 shows the Whisker plot of modeled (a) Hs (b) Tp and (a) θ of each season, from 1980 to 2018. The observed (and transferred) average and extreme wave conditions, which were obtained from the CC & CRMD, are also shown in Fig. 12. The observed and model values followed the same pattern. The reasons for the difference in Hs and Tp could be attributed to wave transformation errors and wave shoaling effects.

Fig. 12. Whisker plot diagrams (a) H_s, (b) T_p, and (c) θ of each season since 1980 to 2018; and the average and extreme wave conditions, based on transformed wave data

Fig. 13 (a) shows the time series data of H_s (from January 1, 1980, to January 1, 2019) and its moving average over 365 days (1 year). Relatively high waves occurred during the southwest monsoon. For a gradient of 1 year, the moving average was 5×10^{-5} ($R^2 = 0.1123$). The 1-year moving average plot did not show a significant fluctuation in H_s. Fig. 13 (b) shows the Whisker plot diagram for all H_s values in the range of high waves. Therefore, we further analyzed the high waves as well as the long waves.

Fig. 13. (a) Significant wave heights (Hs) and its 365-day moving average, (b) Whisker plot diagram of Hs and the definition of high waves

Fig. 14 (a) shows the percentage of days of long waves in each year. Long-wave days were defined in a similar way as high-wave days by plotting the time series of all peak wave periods (Tp). The third quartile (Q3) of all Tp values was 5.8 s. The percentage of long-wave days did not change from 1980 to 2018. Fig. 14 (b) depicts the percentage of days with high waves for each year. The results reveal that a relatively higher percentage of high waves occurred after 2012. Fig. 14 (c) illustrates the percentage of high waves for different direction groups. North is defined as 0° and all directions are relative to north. Most of the high waves were reached from the 240°–250°, 250°–260°, 260°–270°, and 270°–280° wave directions. The results reveal that the high waves approaching from the 240°–250° (0.0002, $R^2 = 0.34$) and 250°–260° (0.0013, $R^2=0.26$) direction groups exhibit an increasing trend, while high waves approaching from 260°–270° (0.0004, $R^2=0.01$) and 270°–280° (−0.0004, $R^2=0.04$) do not show an increasing trend. The regression coefficients and R-squared values are displayed within the brackets. Due to increased high-wave conditions associated with climate change, nourished sand moved off-shoreward and in the northward direction (Q_{Out}).

Fig. 14. (a) Percentage of long-wave days for each year, (b) percentage of days of high waves for each year, and (c) percentage of reached high waves in selected direction groups (230°–240°, 240°–250°, 250°–260°, 260°–270°, 270°–280°, 280°–290° and 290°–300°)

3.6 Sediment transport flux

$Q_{\mathrm{Out\_max}}$ is the capacity of littoral drift due to wave climate. Q_{Out} is the actual sediment outflux, whose upper limit is $Q_{\mathrm{Out\_max}}$. Fig. 15 (a) compares the volume of net annual littoral drift ($Q_{\mathrm{Out\_max}}$), which was calculated from both formulas. The CERC formula estimates a relatively high sediment transport volume. These values are not consistent with the sediment transport studies of 1992 and 2007 (Fittschen, Perera, and Scheffer, 1992; Samarawikrama et al., 2009). Therefore, Fig. 15-(b) shows only the $Q_{\mathrm{Out\_max}}$ estimations from the Kamphuis formula, which was more realistic, considering field survey results and interviews. The positive littoral drift indicates northward sediment transport, while the negative littoral drift indicates southward transport. The results reveal that the sediment transport of the littoral drift increased after 2012, and values reached extremes in 2017. Although the littoral drift has the capacity to transport $Q_{\mathrm{Out\_max}}$ sediments, it cannot easily erode the western coast (between Colombo port and MB) as the entire coastline is protected through the detached breakwater, revetments, and groins. The littoral drift could erode areas of Marawila where beach nourishment is undertaken.

Fig. 15. Comparison of estimated volumes of littoral drift along MB from (a) CERC (with Kamphuis for comparison) and (b) Kamphuis formula from 1980 to 2018

Beach nourishment (mainly in Zone B and Zone D) was rapidly eroded by the littoral current. A portion of the transported sand was held by the groin field in Zone E. Fig. 16 shows photographs that were taken in Zone B and E after beach nourishment was performed and show evidence of the northward transport of sediment due to the severe southwest monsoon wave climate of 2017.

Fig. 16. Beach nourishment near a hotel in Zone B. (Photographs taken on (a) February 13, 2017; (b) August 1, 2017; (c) February 28, 2018; and (d) February 21, 2019.) Shoreline near a pink-colored church in Zone E (Photographs were taken on (e) December 19, 2016; (f) August 1, 2017; (g) February 21, 2018; and (h) February 21, 2019)

3.7 Spatio-temporal change in beach sediment volume in northern cell

As there were no good quality satellite images to extract shoreline with the required accuracy of 10 m before 2001, the authors extracted shoreline only from 2001. This section discusses the status of Q_{Hold}.

After enacting strict regulations of river sand mining in 2004, detached breakwaters were introduced to restore the beach from 2005 to 2010 between the river mouth and MB. Fig. 17 shows (a) the total accretion and erosion and (b) the cumulative sediment accretion between the river mouth and MB (14 km beach stretch) from December 2001 to May 2019. Initially, 12.3 million m^3 (1.23 million m^3/y) was accumulated during 2004–2014. The accreted area eroded later at a rate of 1.55 million m^3/y due to intensified wave conditions [see Fig. 14 (b)]. The detached breakwaters effectively captured sediment but caused massive erosion downcoast of MB as a result of the interruption of the northward littoral drift. However, the accreted shore was slowly eroded after 2010.

Fig. 17. (a) Spatial extent between Maha River and MB (Image was taken in February 2017) (Source: Google Earth, Data SIO, NOAA, U.S. Navy, NGA, GEBCO) (Image was taken by DigitalGlobe); (b) total sediment accretion between the Maha River mouth and Marawila during December 2001 to May 2017; (c) cumulative accretion between the Maha River mouth and MB from December 2001 to May 2019

3.8 Spatio-temporal change in beach sediment volume in southern cell and its management

This section discusses the status of Q_{Erosion}. Spatio-temporal changes (from 2002 to 2017) in the beach area at MB have been studied by Samarasekara et al. (2018). We have investigated the spatio-temporal changes in 2018 and 2019. Fig. 18 shows the cumulative accretion of the beach volume in MB from 2001 to 2019. The beach volume increased due to the beach nourishment during December 2016 and February 2017. The accretion (and erosion) in the southern and northern cells are shown in Fig. 17 (c) and Fig. 18, respectively. Typical protection measures in the northern and southern cells were beach nourishment and installation of detached breakwaters, respectively. The nourished beach in the northern cell was, however, continuously eroded due to severe monsoon waves, while the breakwaters in the southern cell efficiently restored the beach.

Fig. 18. Cumulative beach volume accretion (negative values denotes the erosion) of MB from 2001 to 2019

Table 4 shows the accreted beach area, change in beach slope (spatially averaged slope), and cost of adopted measures in each zone studied. Adopted measures in Zone C are effective in restoring the beach area and reducing the beach slope; however, this seems to be the most expensive adopted measure. In the early 1980s, the supply of river sand was drastically reduced it was difficult to reinstate river sand flow. The most appropriate sustainable solution to maintain MB is seasonal beach nourishment. However, with the intensified wave conditions, the nourished beach would be eroded. Therefore, a combination of beach nourishment and detached breakwater seems the most suitable adopted measure. Management measures for each zone are shown in Table 4. The cost of a detached breakwater, submerged breakwater, and groin was 1.31 million USD (United States Doller), 0.41 million USD, and 0.28 million USD, respectively. The length scale information is shown in Table 2. The cost of offshore sand (which was used for beach nourishment) was 11 USD/m^2. The cost of a unit length of a revetment was 342 USD/m.

Table 4. Accreted beach area, change in beach slope, cost of adopted measures and cost to grow a unit beach area in each zone between February 2017 and February 2018

	Zone A	Zone B	Zone C	Zone D	Zone E
Accreted beach area (m^2/m)	8	-88	118	-253	158
Change in beach slope (%)	38.9	-6.9	0	-3.8	14.3
Cost (USD/m)	591	2161	2390	1995	314
Cost to grow an unit beach area (USD/ m^2)	74	-	20	-	2

As Zone B and C were still eroding, the cost of growing a unit area was not defined in Table 4. Table 4 shows that the cost of preventing erosion without beach nourishment (in Zone A) was nearly four times (=76/20) higher than that with beach nourishment (in Zone C). Beach nourishment is continuous, and Table 4 only reflects a short time period of 1-3 years. The annual budget to manage 1340 km of total shoreline in Sri Lanka was 5.8 million USD in 2017 (MMDE, 2018). The cost of beach nourishment was 5.2 million USD, and the allocated budget for 1-year rehabilitation was not sufficient. Therefore, beach nourishment was phased; Stage 1 was completed in 2016, at a cost of 3.2 million USD, while Stage 2 was completed in 2017, at a cost of 2 million USD. Implementation of continuous beach nourishment is difficult with such limited budgets.

3.9 Mechanism of erosion

Fig. 19 shows sediment flux before erosion in MB, during the first decade of erosion, and during the second decade of erosion. Arrows indicate the magnitude of the sediment flux. Sediment flux in 1980–2000, 2000–2010, and 2010-2019 represents the time before erosion, the first decade of erosion, and the present situation, respectively. The sediment flux was obtained from the literature and the analysis focused on the period between 1980 and 2019. The interruptions of littoral drift from the detached breakwaters in the river mouth and MB led to erosion at MB. As the entire west coast between Colombo Port and MB was protected by revetments, detached breakwaters, coves, and groins, the beach was protected from significant erosion. As a result, the littoral drift (Q_{In}) has reduced. Table 5 summarizes the causes of erosion in each decade.

Fig. 19. Sediment flux within the coastal cell including MB and Maha River mouth (a) before erosion in (1980–2000) (b) first decade of erosion (2000–2010) (c) during second decade of erosion (2010-2019) in MB

Table 5. Causes of erosion in each decade at northern cell (MB) and southern cell

Decade	Causes of erosion
1980 – 2000	Southern cell: Coast protection from detached breakwaters, groins and revetments in sediment upstream, reduction in sediment supply from Kalani river and Negombo lagoon mouth, Construction of barrage over Maha river, sand mining in Maha river; Northern cell: No erosion
2000 – 2010	Southern cell: No erosion; Northern cell: Coast protection from detached breakwaters and groins in southern cell, excessive clay and illegal sand mining in Maha river riparian
2010 – 2019	Southern and northern cells: Intensified wave climate

Continuous beach nourishment is required to maintain a wide sandy beach. The apparent solution is beach nourishment combined with hard engineering structures, such as detached breakwaters and groins. However, these solutions are costly, thus exerting a heavy financial burden on the government. A detailed cost-benefit analysis is required for continuous beach nourishment compared to other potential solutions, such as (i) covering the entire coast with detached breakwaters, (ii) implementing a mega beach nourishment program upstream (near the river mouth), (iii) managing mass relocation (retreat), and (iv) replacing all barrages and dams with automated gates, which allow sediment bypass from inland rivers. For example, Taiwan is a country that covered its entire coastline line with coast protection measures (Chiang et al., 2017). Mega beach nourishment has been successful in the Netherlands (Pit, Griffioen and Wassen, 2017; Luijendijk et al., 2018). Mega relocation measures have been implemented in developed countries in

Europe (McCreary et al., 2001) and in developing countries such as Ghana (Jonah, 2015) and Senegal (Ndour et al., 2018).

Due to the limited budget in developing countries, it is necessary to invest more in long-term and large-scale solutions. There is a need for further research on the status and mechanism of beach erosion in order to support decision-making regarding investment in engineered coastal protection measures.

4. Conclusions

Coastal erosion on the west coast of Sri Lanka has been a long-term problem, since the 1980s. The beach area between the Maha River mouth and MB had initially been eroded due to the reduction in the supply of river sand as a result of river sand mining and barrage construction over the river during 1980–2004. Detached breakwaters were introduced between the river mouth and MB during 2005–2010, and as a result, the beach was severely eroded. To protect MB, various hard and soft measures, such as submerged breakwaters, detached breakwaters, revetments, and beach nourishment have been implemented during 2011–2016. Beach nourishment was conducted using offshore sand at the end of 2016; however, it was only effective when combined with detached breakwaters and groins. This combination effectively restored the beach and recovered the original beach slope, which had been steepened during the rough monsoon season in 2017. Beach nourishment is an expensive measure and will not always be affordable for the government of Sri Lanka. The wave climate intensified after 2011, and the capacity of northward littoral drift increased to an average of 10.6 m^3/y. Moving sediment flux into sediment cells from upstream of the river drastically declined to 0.05 m^3/y due to upstream, illegal clay and sand mining in the river riparian zone. Due to this imbalance in the sediment flux, the unprotected (and nourished) MB has been significantly eroded in recent years. The lack of integration in MB and the entire sediment system is a major issue; thus, it is necessary to study the feasibility of long-term solutions to prevent erosion. In this study, we empirically analyzed all available and quantifiable data related to the erosion problem in MB. Moreover, we hope that this study can contribute to engineering and management data on sustainable coastal erosion management in developing countries to improve the mitigation of coastal erosion hazards.

Disclosure statement

No potential conflict of interest was reported by the authors.

References

Aedla R, Dwarakish GS, Reddy DV (2015) Automatic Shoreline Detection and Change Detection Analysis of Netravati-GurpurRivermouth Using Histogram Equalization and Adaptive Thresholding Techniques. Aquat Procedia 4:563–570. doi: 10.1016/j.aqpro.2015.02.073

Bamunawala RMJ, Hettiarachchi SSL, Samarawickrama SP, et al (2015) Climate Change Impacts on Seasonal Wave Climate of the Western Coast of Sri Lanka. ACEPS 2015 pp. 126

CC&CRMD (2006) Coastal Zone Management Plan (CZMP) 2004. In: Gaz. Extraordinary Part I Sec Gaz. Extraordinary Democr. Social. Repub. Sri Lanka 2006. http://www.coastal.gov.lk/downloads/pdf/CZMP English.pdf. Accessed 9 Oct 2017

CECB (2015) Proposed Colombo Port City Development Project, Colombo, Sri Lanka Supplementary Environmental Impact. Colombo,Sri Lanka, pp 12–16

Chawla A, Tolman HL (2007) Automated grid generation for WAVEWATCH III, pp 71 https://polar.ncep.noaa.gov/mmab/papers/tn254/MMAB_254.pdf. Accessed 18 Dec 2018

Chiang YC, Fang HM, Hsiao SS, Wang HY (2017) Approaching Taiwan's coastal management problems from the perspective of Toucheng Beach's disappearance. Ocean Coast Manag 146:170–177. doi: 10.1016/j.ocecoaman.2017.07.004

Dayananda H V (1992) Shoreline Erosion in Sri Lanka's Coastal Areas. Coast Conservation Department, Colombo,Sri Lanka, pp 25-42

Fernando MSN (2009) Application of Mathematical Modelling for Predicting Coastal Evolution. Dissertation,The University of Moratuwa, Sri Lanka

Fittschen T, Perera JASC, Scheffer H. (1992) Sediment transport study for the Southwest Coast of Sri Lanka. Colombo,Sri Lanka

Gari SR, Newton A, Icely JD (2015) A review of the application and evolution of the DPSIR framework with an emphasis on coastal social-ecological systems. Ocean Coast Manag 103:63–77. doi: 10.1016/j.ocecoaman.2014.11.013

Godage D (1992) Coast Erosion Management Plan and It's Implementation. In: Scheffer H. (ed) Seminar on causes of coastal erosion in Sri Lanka. CCD/GTZ Coast Conservation Project, Colombo,Sri Lanka, pp 323–330

Gunaratna PP, Ranasinghe DPL, Sugandika TAN (2011) Assessment of nearshore wave climate off the Southern Coast of Sri Lanka. Engineer 44:33–42. doi: 10.4038/engineer.v44i2.7021

Hager WH (1987) Lateral outflow over side weirs. J Hydraul Eng 113:491–504.

Ranasinghe I; Banda RMR (1992) Monitoring Resource Utilization and Their Impacts in the Coastal Zone. In: H.J Scheffer (ed) Seminar on Causes of Coastal Erosion in Sri Lanka. Colombo,Sri Lanka, pp 269–288

Jonah FE (2015) Managing coastal erosion hotspots along the Elmina, Cape Coast and Moree area of Ghana. Ocean Coast Manag 109:9–16. doi: 10.1016/j.ocecoaman.2015.02.007

Kalnay E, Kanamitsu M, Kistler R, et al (1996) The NCEP/NCAR 40-year reanalysis project. Bull Am Meteorol Soc 77:437–472.

Kamaladasa B (2008) Issues and challenges in river management due to excessive sand mining. In: River Symposium - International Water Centre. Melbourne, Australia, p 11

Karunaratne W (2011) Impacts of Sand and Clay Mining on the Riverine and Coastal Ecosystems of the Maha Oya : Legal and Policy Issues and Recommendations. Colombo, Sri Lanka, pp 11-12

Lloyd MG, Peel D, Duck RW (2013) Towards a social–ecological resilience framework for coastal planning. Land Use Policy 30:925–933. doi: https://doi.org/10.1016/j.landusepol.2012.06.012

Luijendijk A, Hagenaars G, Ranasinghe R, et al (2018) The State of the World's Beaches. Sci Rep 8, 6641:1–11. doi: 10.1038/s41598-018-24630-6

McCreary S, Gamman J, Brooks B, et al (2001) Applying a Mediated Negotiation Framework to Integrated Coastal Zone Management. Coast Manag [previously Coast Zo Manag J] 29:183–216. http://doi: 10.1080/08920750152102035

MMDE (2018) Annual Performance Report Accounts 2017. Colombo,Sri Lanka, pp 40 http://www.parliament.lk/uploads/documents/paperspresented/performance-report-ministry-of-mahaweli-development-environment-2017.pdf. Accessed 10 Oct 2010

NARA (2007) CCD-ChilawBathymetry [.dwg file]. Colombo: CC & CRMD. Available at Chief Engineer's Office (Coastal Development), Coast Conservation & Coastal Resource Management Department, Colombo, Sri Lanka [accessed 2017 February 23]

Ndour A, Laïbi RA, Sadio M, et al (2018) Management strategies for coastal erosion problems in west Africa: Analysis, issues, and constraints drawn from the examples of Senegal and Benin. Ocean Coast Manag 156:92–106. doi: https://doi.org/10.1016/j.ocecoaman.2017.09.001

NGDC (2006) 2-minute gridded global relief data (ETOPO2) v2. doi: 10.7289/V5J1012Q

Oertel GF (2005) Coasts, Coastlines, Shores, and Shorelines. In: Schwartz ML (ed) Encyclopedia of Coastal Science. Springer Netherlands, Dordrecht, pp 323–327

Perera HN. (1990) Need for review and upgrading of master plan for coast erosion management. In: Sheffer HJ (ed) Seminar on Causes of Coastal Erosion in Sri Lanka. CCD/GTZ Coast Conservation Project, Colombo, Sri Lanka, pp 331–348

Pit IR, Griffioen J, Wassen MJ (2017) Environmental geochemistry of a mega beach nourishment in the Netherlands: Monitoring freshening and oxidation processes. Appl Geochemistry 80:72–89. doi: https://doi.org/10.1016/j.apgeochem.2017.02.003

Pranzini E (2018) Shore protection in Italy: From hard to soft engineering … and back. Ocean Coast Manag 156:43–57. doi: 10.1016/j.ocecoaman.2017.04.018

Rangel-Buitrago N, Williams AT, Anfuso G (2018) Hard protection structures as a principal coastal erosion management strategy along the Caribbean coast of Colombia. A chronicle of pitfalls. Ocean Coast Manag 156:58–75. doi: 10.1016/j.ocecoaman.2017.04.006

Saengsupavanich C (2013) Detached breakwaters: Communities' preferences for sustainable coastal protection. J Environ Manage 115:106–113. doi: 10.1016/j.jenvman.2012.11.029

Saengsupavanich C, Chonwattana S, Naimsampao T (2009) Coastal erosion through integrated management: A case of Southern Thailand. Ocean Coast Manag 52:307–316. doi: 10.1016/j.ocecoaman.2009.03.005

Samarasekara RSM, Sasaki J, Jayaratne R, et al (2018) Historical changes in the shoreline and management of Marawila Beach, Sri Lanka, from 1980 to 2017. Ocean Coast Manag 165:370–384. doi: 10.1016/j.ocecoaman.2018.09.012

Samarasekara RSM (2019) Evaluation of Coastal Erosion Processes and Management in a Developing Country: A Case Study in Marawila Beach, Sri Lanka. Dissertation, The University of Tokyo, Japan

Samarawikrama SP, Costa WAJ, Dissanayaka DMB, Dulshan PR. (2009) Coastal Erosion Management in Sri Lanka. Dissertation, University of Moratuwa, Sri Lanka

Schmidt L, Gomes C, Guerreiro S, O'Riordan T (2014) Are we all on the same boat? The challenge of adaptation facing Portuguese coastal communities: Risk perception, trust-building and genuine participation. Land Use Policy 38:355–365. doi: 10.1016/j.landusepol.2013.11.008

Thevasiyani T, Perera K (2014) Statistical analysis of extreme ocean waves in Galle, Sri Lanka. Weather Clim Extrem 5: 40–47.

Tolman HL (2009) User manual and system documentation of WAVEWATCH III TM version 3.14. Tech note, MMAB Contrib 276:220 https://polar.ncep.noaa.gov/mmab/papers/tn254/MMAB_254.pdf. Accessed 18 Dec 2018

Van Rijn LC (2003) Longshore sand transport. In: Coastal Engineering 2002: Solving Coastal Conundrums. World Scientific, pp 2439–2451

Van Rijn LC (2013) Simple general formulae for sand transport in rivers, estuaries and coastal waters. pp 1–16. https://www.leovanrijn-sediment.com/papers/Formulaesandtransport.pdf. Accessed 4 Jul 2019

White A, Deguit E, Jatulan W, Eisma-Osorio L (2006) Integrated coastal management in Philippine local governance: Evolution and benefits. Coast Manag 34:287–302. doi: 10.1080/08920750600686687

Wickramaarachchi B (2011) Spatial Analysis & Mapping, Maha Oya Lowland Corridor. Colombo,Sri Lanka, pp 16-17

Williams AT, Rangel-Buitrago N, Pranzini E, Anfuso G (2018) The management of coastal erosion. Ocean Coast Manag 156:4–20. doi: 10.1016/j.ocecoaman.2017.03.022

Yin P, Duan X, Gao F, et al (2019) Coastal erosion in Shandong of China: status and protection challenges. China Geol 1:512–521. doi: 10.31035/cg2018073

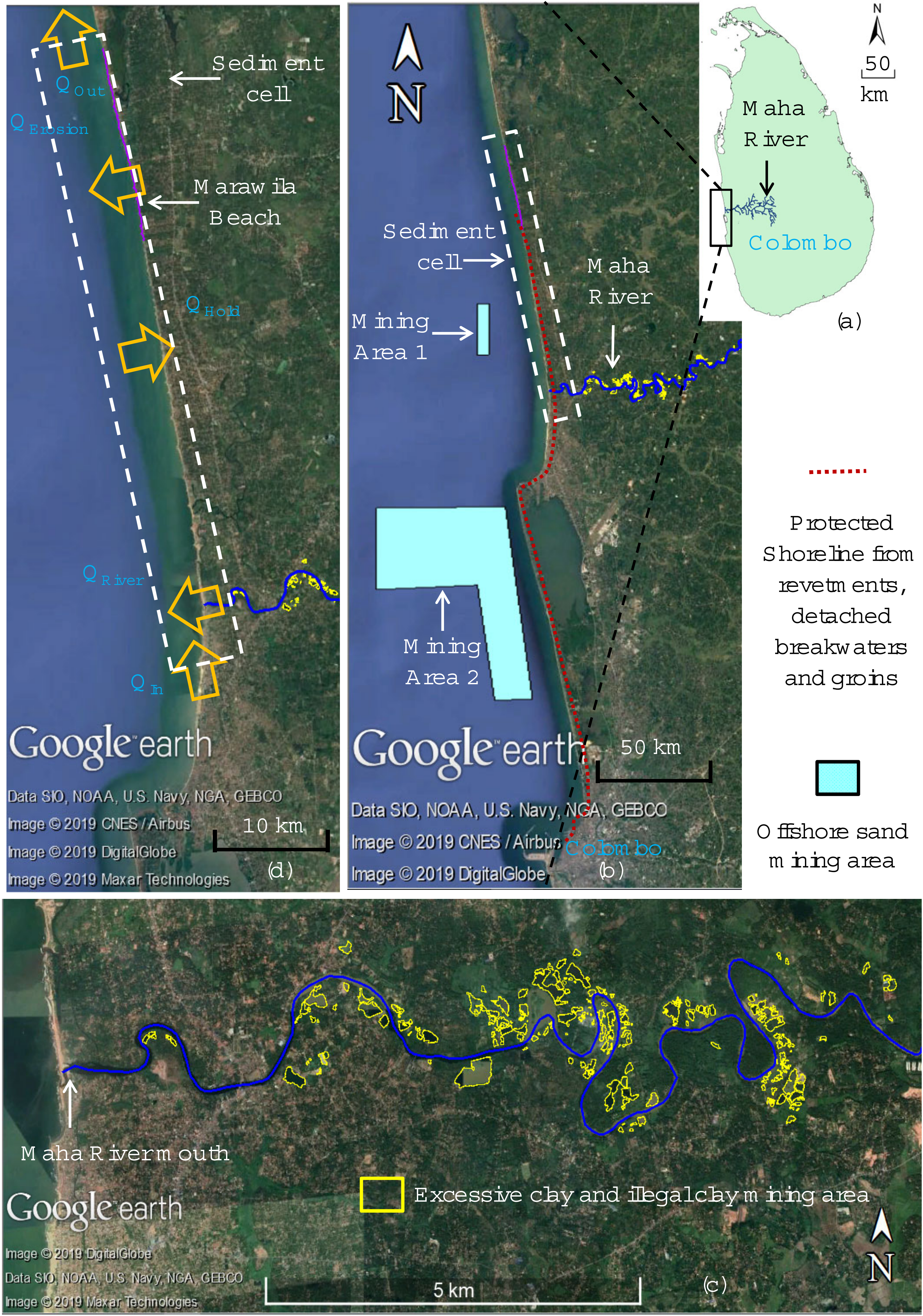

Sediment cell
Q Out
Q Erosion
Marawila Beach
Q Hold
Q River
Q In
Data SIO, NOAA, U.S. Navy, NGA, GEBCO
Image © 2019 CNES / Airbus
Image © 2019 DigitalGlobe
Image © 2019 Maxar Technologies
10 km
(d)
N
Sediment cell
Mining Area 1
Maha River
Mining Area 2
50 km
Colombo
(b)
50 km
Maha River
Colombo
(a)
Protected Shoreline from revetments, detached breakwaters and groins
Offshore sand mining area
Maha River mouth
Excessive clay and illegal clay mining area
Image © 2019 DigitalGlobe
5 km
(c)

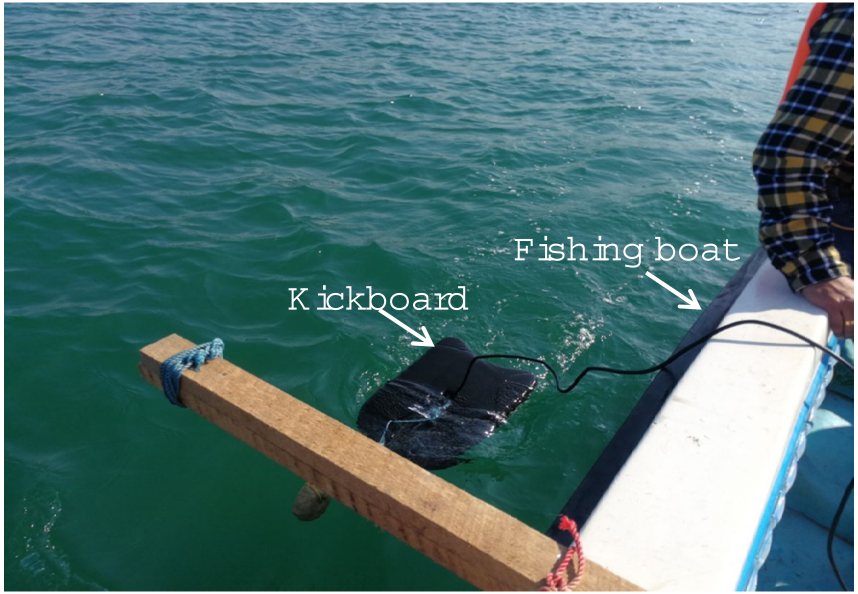
Fishing boat
Kickboard

(a)

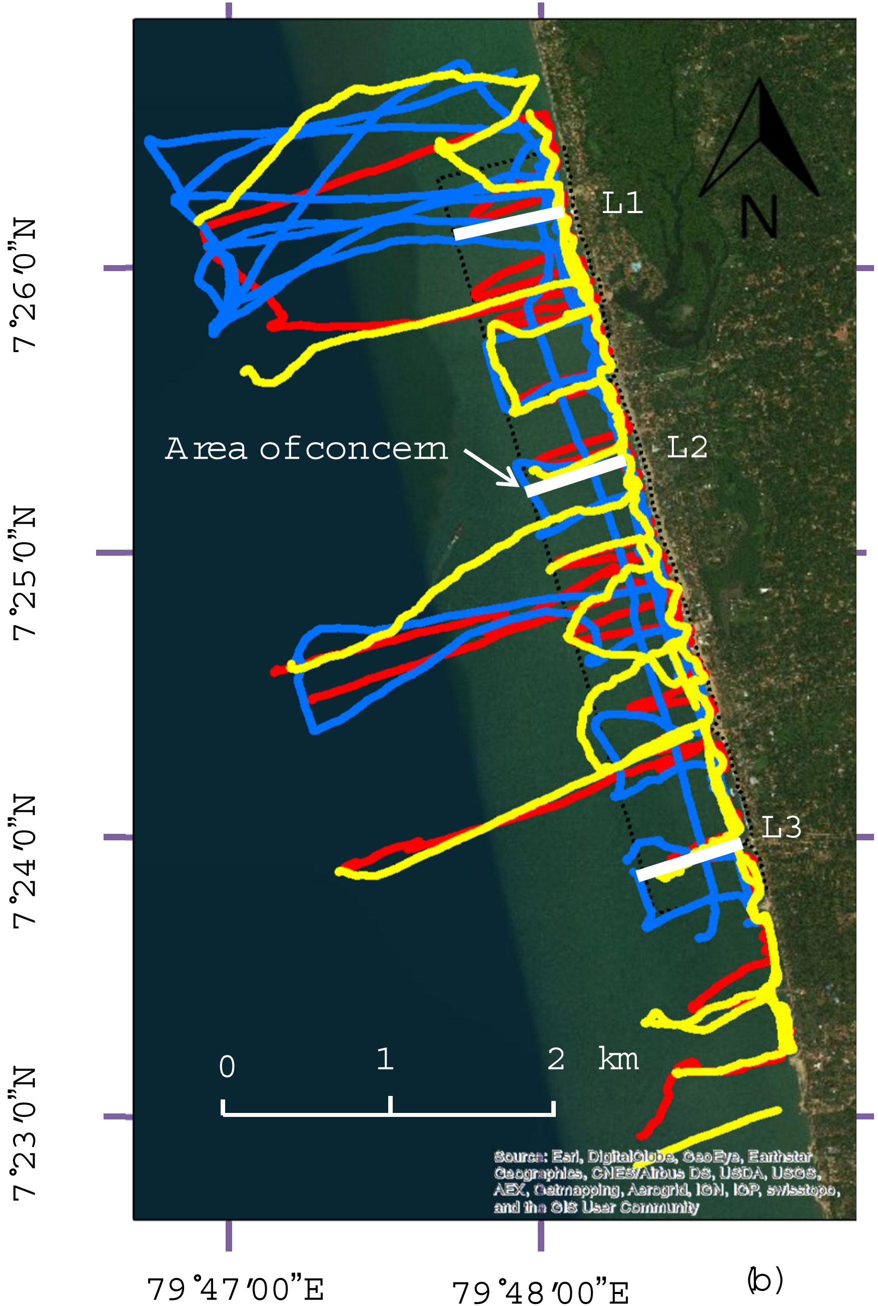
Area of concern
2017-survey tracklines
2018-survey tracklines
2019-survey tracklines
L1
L2
L3
Area of concern
N
0
1
2
km
7°26′0″N
7°25′0″N
7°24′0″N
7°23′0″N
79°47′00″E
79°48′00″E
Source: Esri, DigitalGlobe, GeoEye, Earthstar Geographics, CNES/Airbus DS, USDA, USGS, AEX, Getmapping, Aerogrid, IGN, IGP, swisstopo, and the GIS User Community

(b)

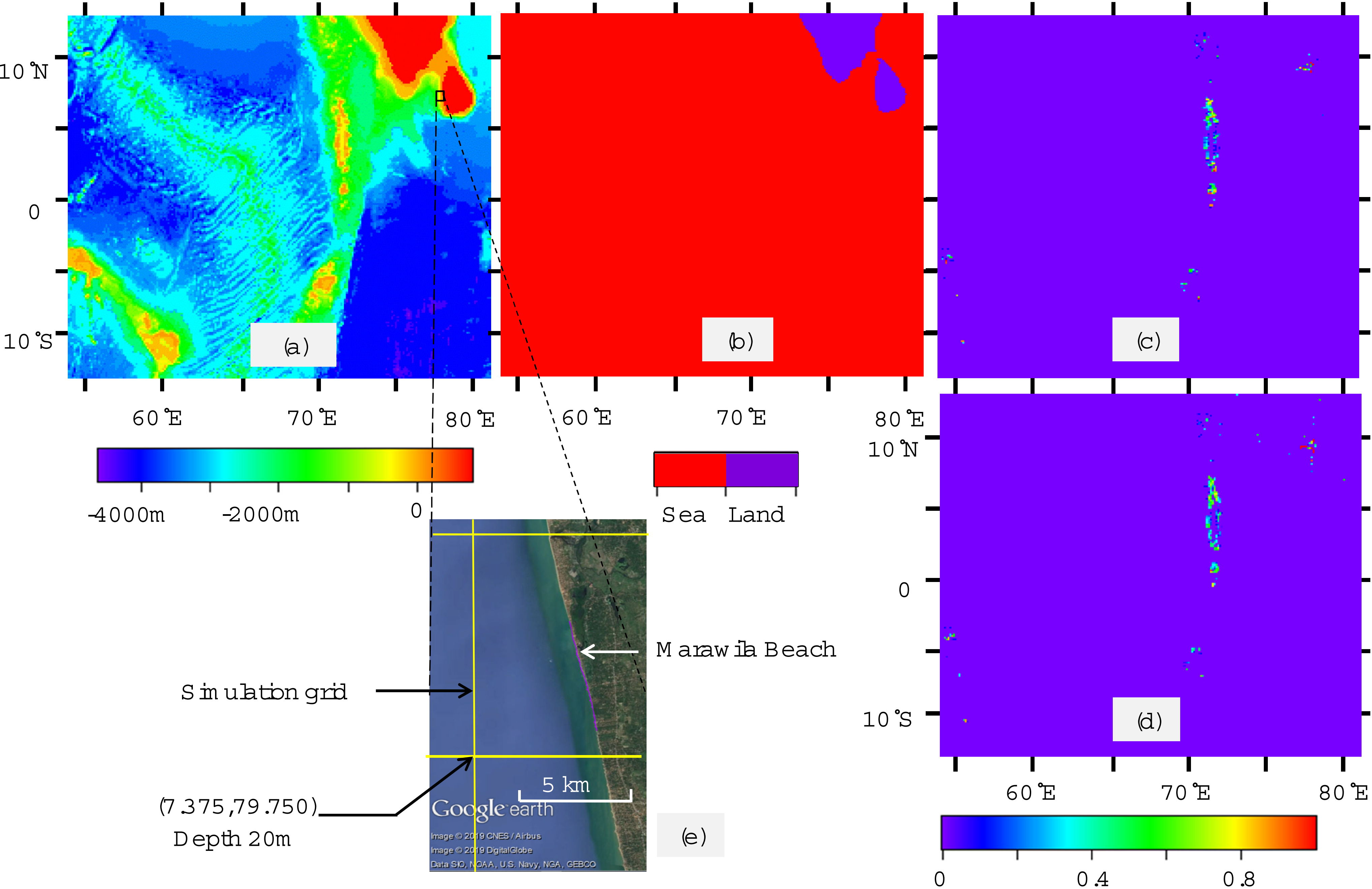

10°N
0
10°S
60°E
70°E
80°E
(a)
(b)
(c)
(d)
(e)
-4000m
-2000m
0
Sea
Land
Marawila Beach
Simulation grid
(7.375,79.750)
Depth 20m
5 km
Google earth
Image © 2019 CNES / Airbus
Image © 2019 DigitalGlobe
Data SIO, NOAA, U.S. Navy, NGA, GEBCO
0
0.4
0.8

(a)

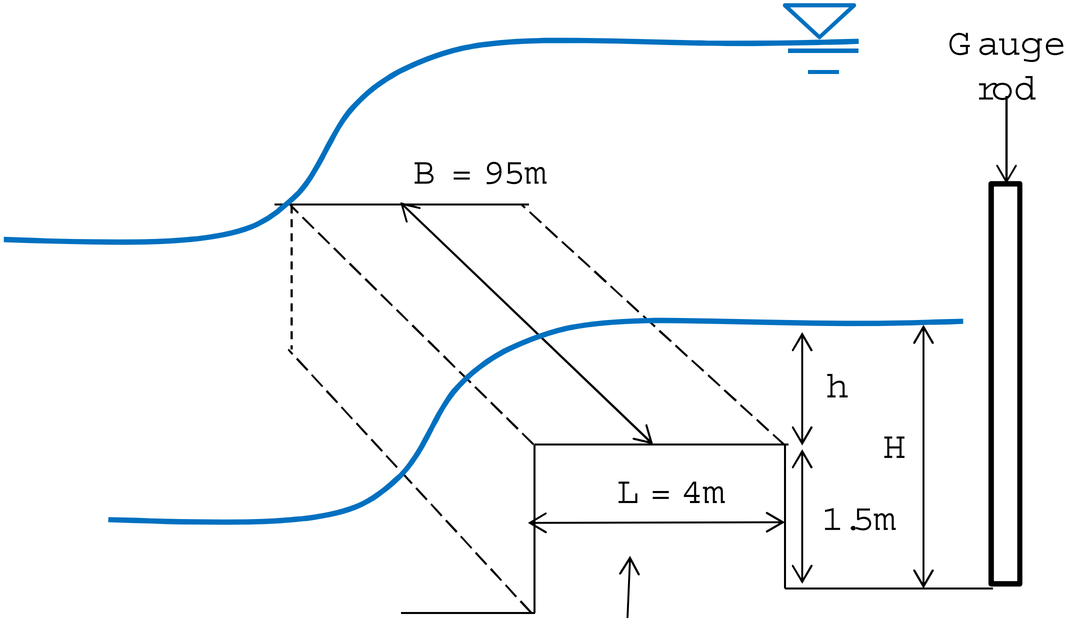

(b)

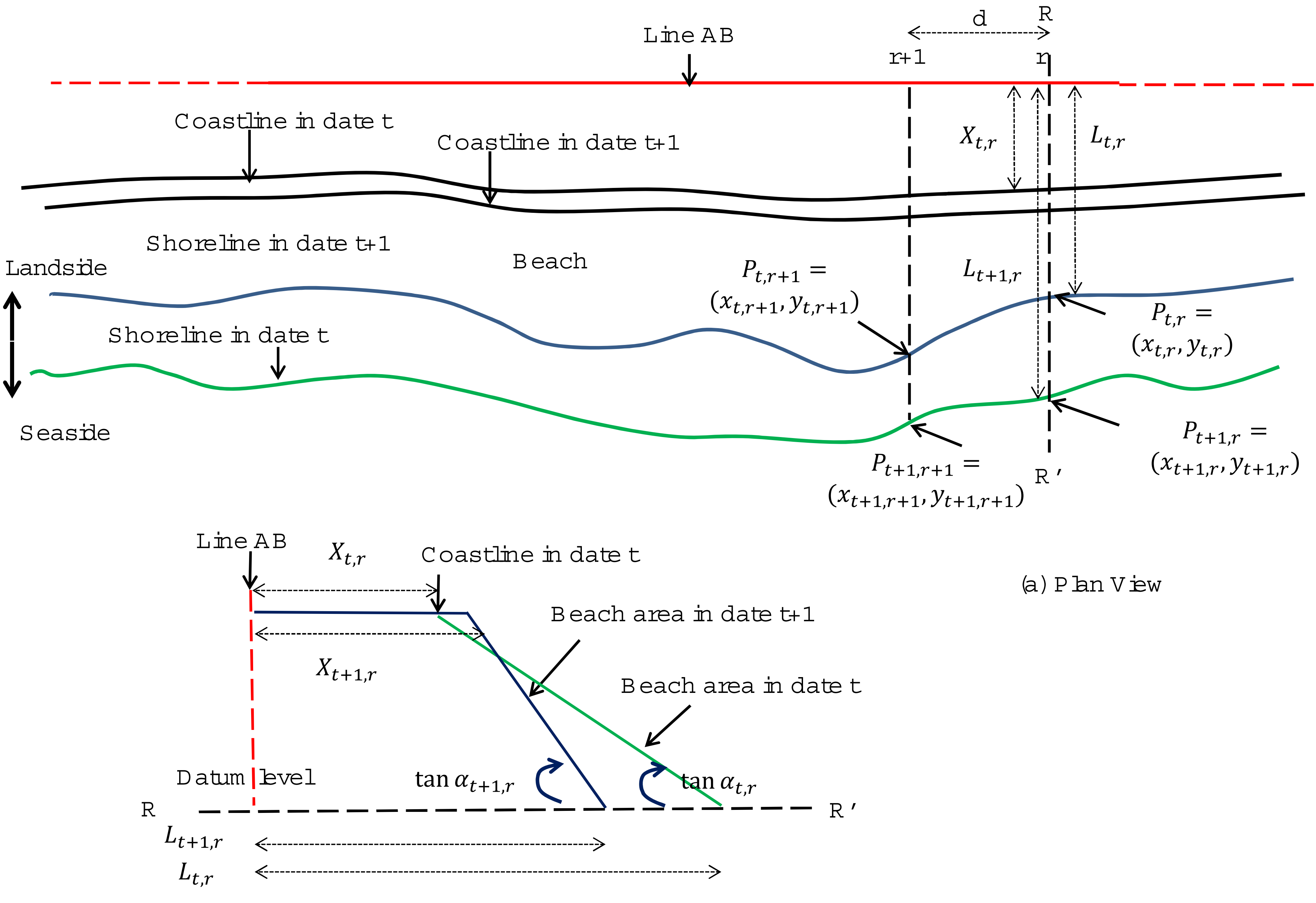

(a) Plan View

(b) Cross-section

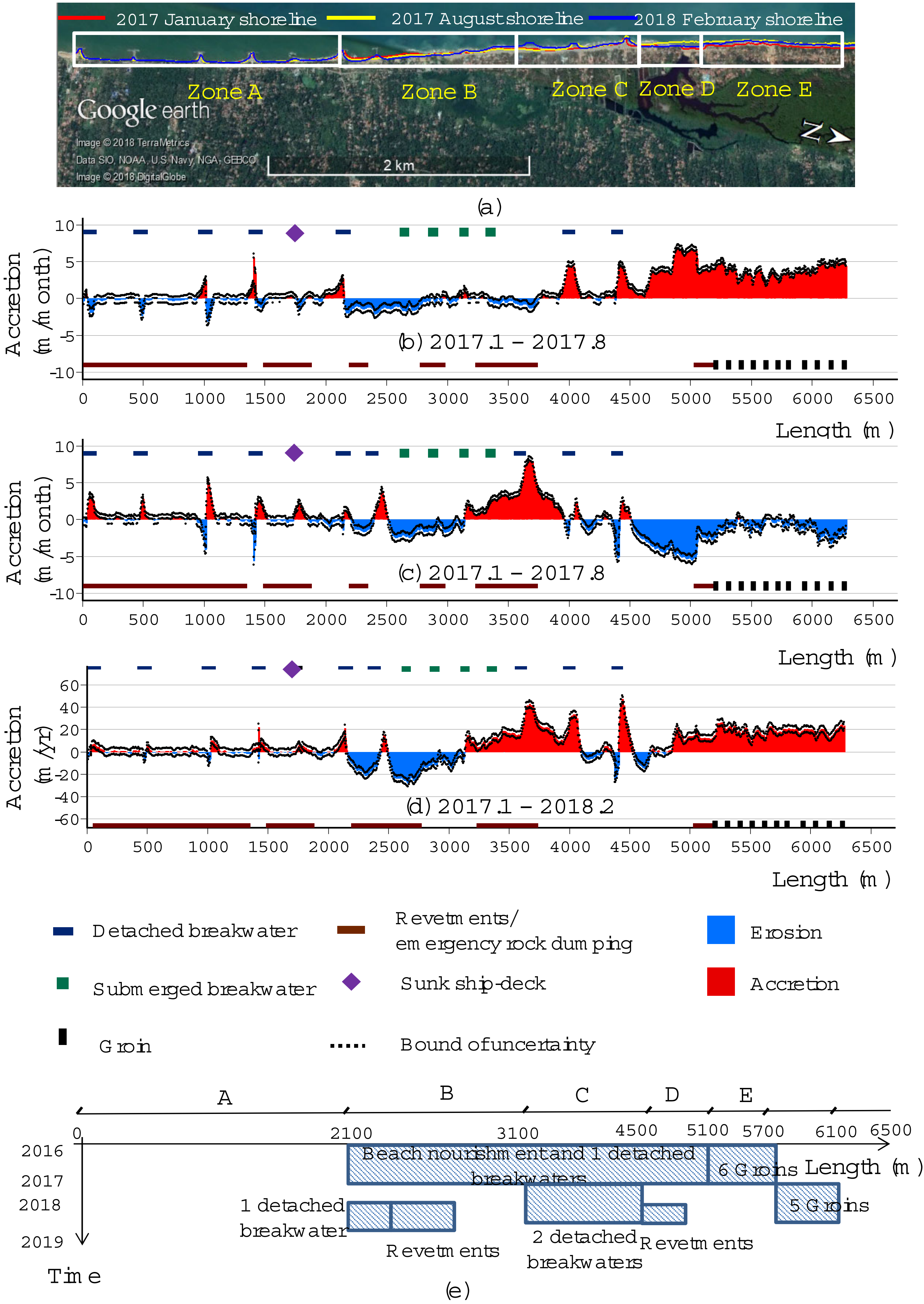

2017 January shoreline
2017 August shoreline
2018 February shoreline
Zone A
Zone B
Zone C
Zone D
Zone E
Google earth
Image © 2018 TerraMetrics
Data SIO, NOAA, U.S. Navy, NGA, GEBCO
Image © 2018 DigitalGlobe
2 km
N
(a)
Accretion (m/month)
(b) 2017.1 – 2017.8
Length (m)
Accretion (m/month)
(c) 2017.1 – 2017.8
Length (m)
Accretion (m/yr)
(d) 2017.1 – 2018.2
Length (m)
Detached breakwater
Revetments/ emergency rock dumping
Erosion
Submerged breakwater
Sunk ship-deck
Accretion
Groin
Bound of uncertainty
A
B
C
D
E
0
2100
3100
4500
5100
5700
6100
6500
Length (m)
2016
2017
2018
2019
Time
Beach nourishment and 1 detached breakwaters
6 Groins
1 detached breakwater
Revetments
2 detached breakwaters
Revetments
5 Groins
(e)

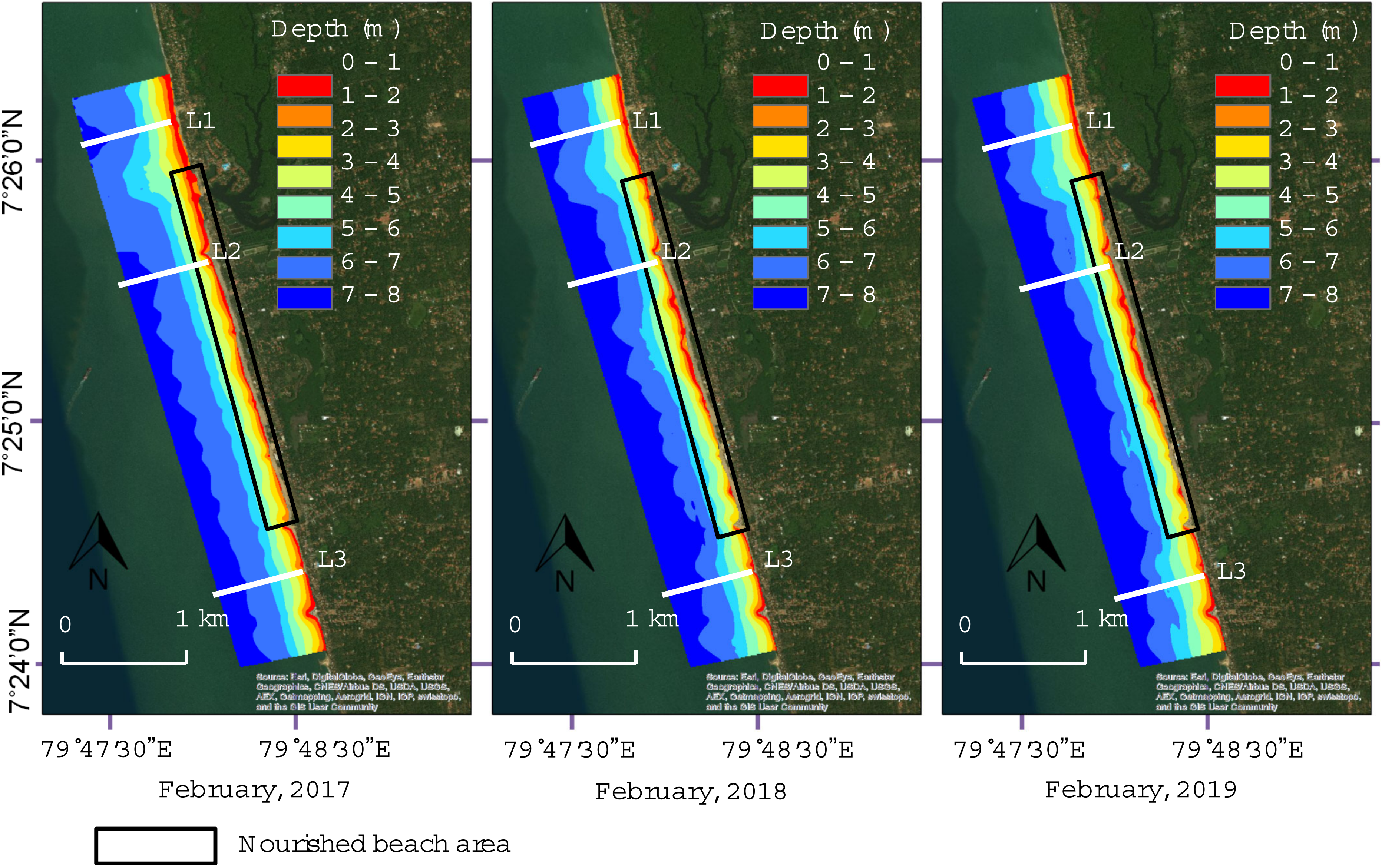

Depth (m)
0 – 1
1 – 2
2 – 3
3 – 4
4 – 5
5 – 6
6 – 7
7 – 8
L1
L2
L3
N
0
1 km
7°26'0"N
7°25'0"N
7°24'0"N
79°47'30"E
79°48'30"E
February, 2017
February, 2018
February, 2019
Nourished beach area

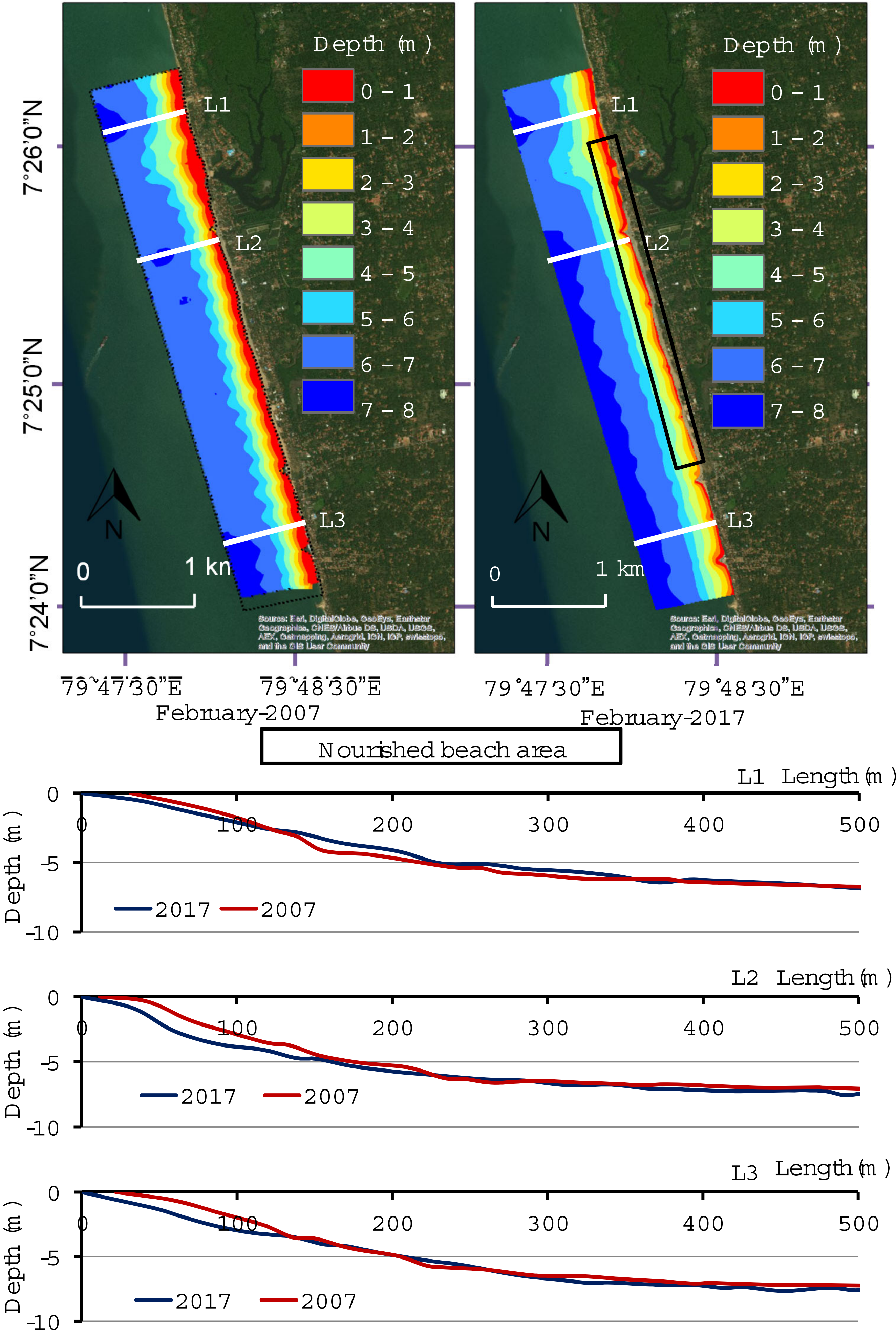
Depth (m)
0 – 1
1 – 2
2 – 3
3 – 4
4 – 5
5 – 6
6 – 7
7 – 8
L1
L2
L3
N
0
1 km
7°26'0"N
7°25'0"N
7°24'0"N
79°47'30"E
79°48'30"E
Source: Esri, DigitalGlobe, GeoEye, Earthstar Geographics, CNES/Airbus DS, USDA, USGS, AEX, Getmapping, Aerogrid, IGN, IGP, swisstopo, and the GIS User Community
February-2007
February-2017
Nourished beach area
L1 Length (m)
L2 Length (m)
L3 Length (m)
0
100
200
300
400
500
Depth (m)
0
-5
-10
2017
2007

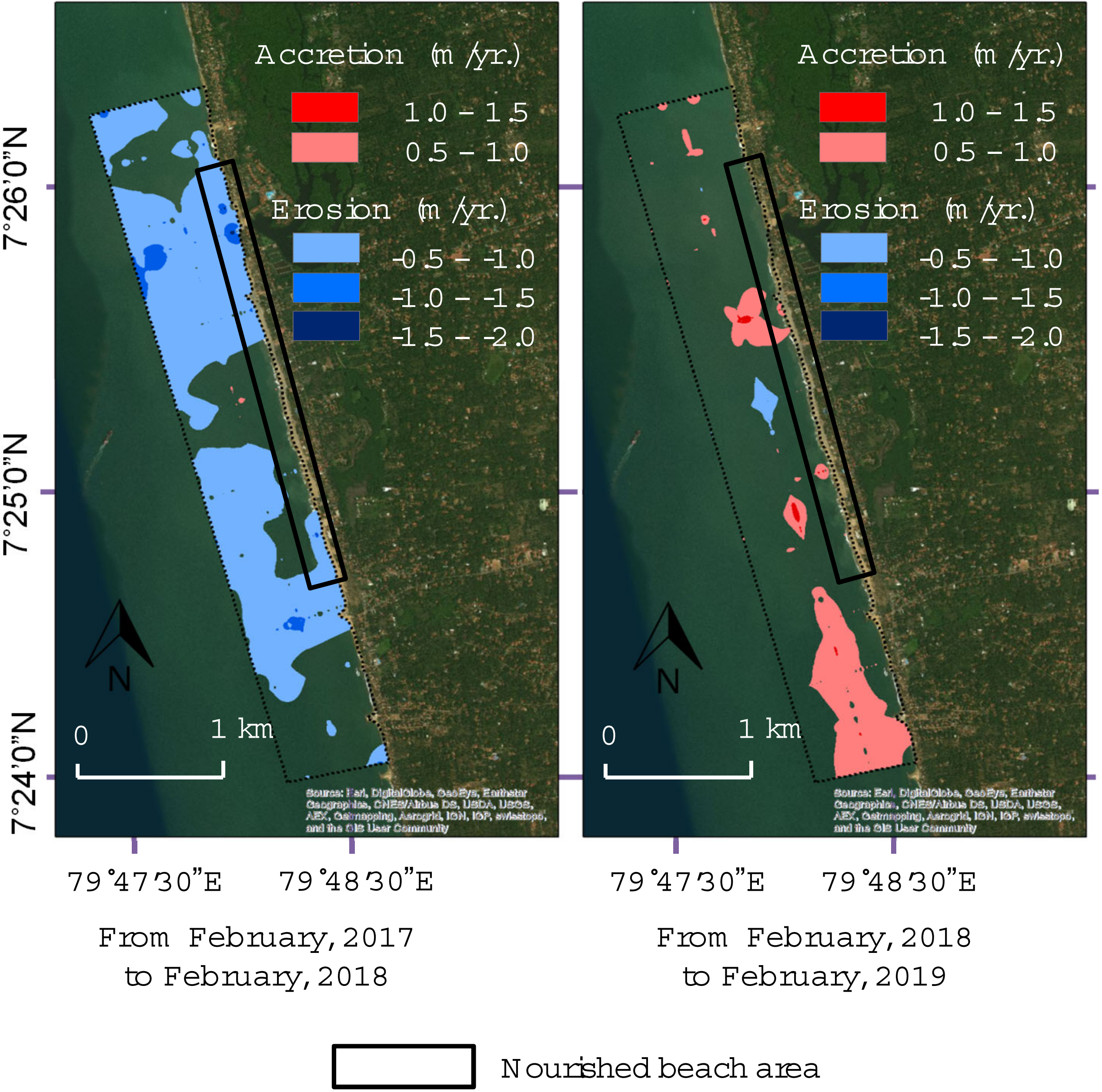

Accretion (m /yr.)
1.0 – 1.5
0.5 – 1.0
Erosion (m /yr.)
-0.5 – -1.0
-1.0 – -1.5
-1.5 – -2.0
N
0
1 km
Source: Esri, DigitalGlobe, GeoEye, Earthstar Geographics, CNES/Airbus DS, USDA, USGS, AEX, Getmapping, Aerogrid, IGN, IGP, swisstopo, and the GIS User Community
7°26'0"N
7°25'0"N
7°24'0"N
79°47'30"E
79°48'30"E
From February, 2017 to February, 2018
From February, 2018 to February, 2019
Nourished beach area

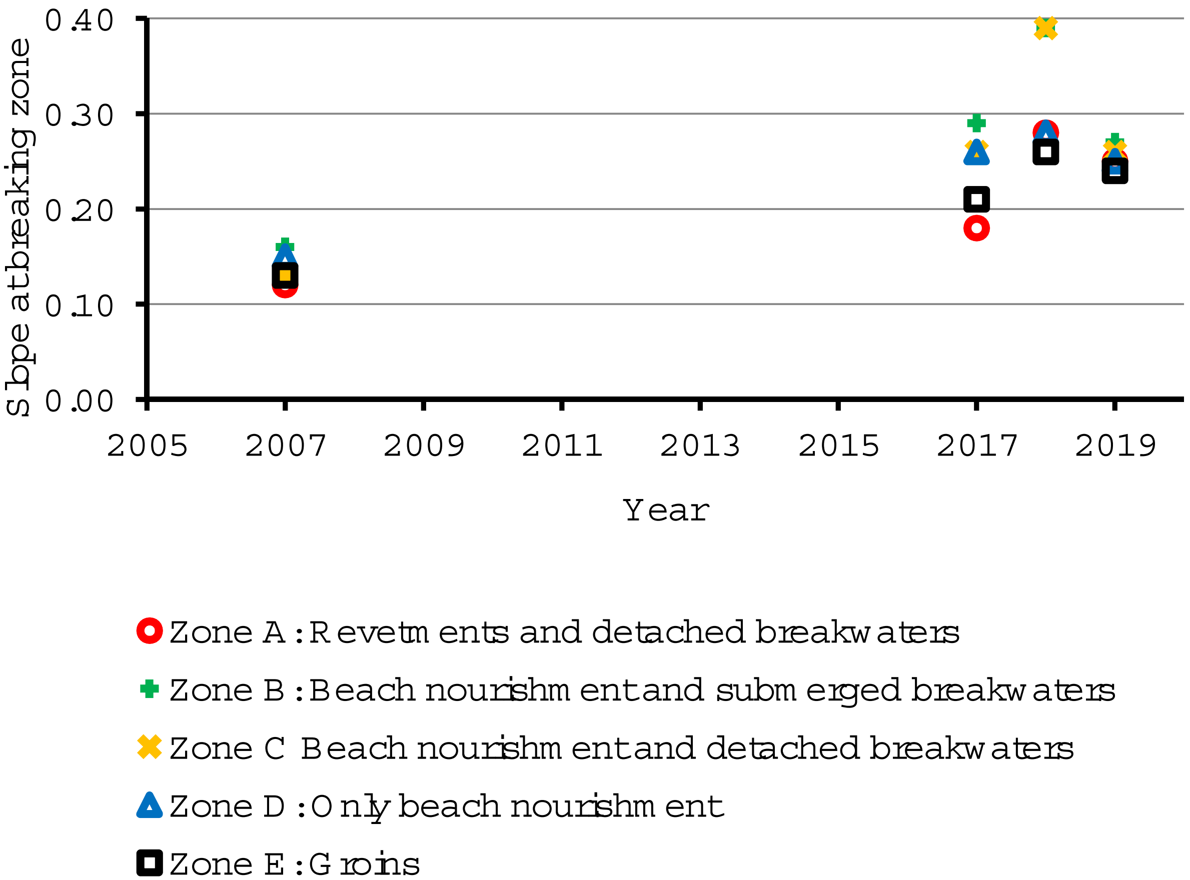

0.40
0.30
0.20
0.10
0.00
Slope at breaking zone
2005
2007
2009
2011
2013
2015
2017
2019
Year
Zone A: Revetments and detached breakwaters
Zone B: Beach nourishment and submerged breakwaters
Zone C Beach nourishment and detached breakwaters
Zone D: Only beach nourishment
Zone E: Groins

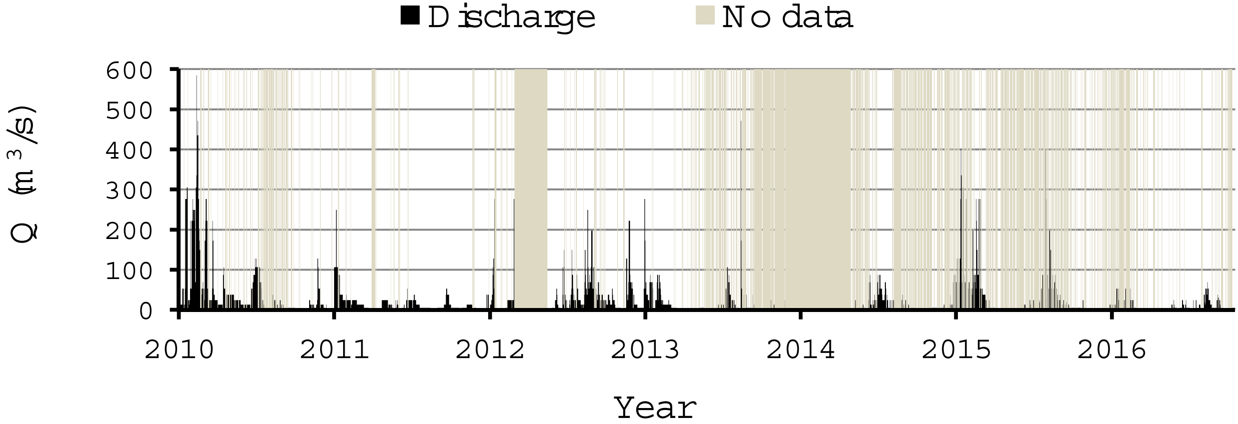

Discharge
No data
Q (m3/s)
600
500
400
300
200
100
0
2010
2011
2012
2013
2014
2015
2016
Year

(a)

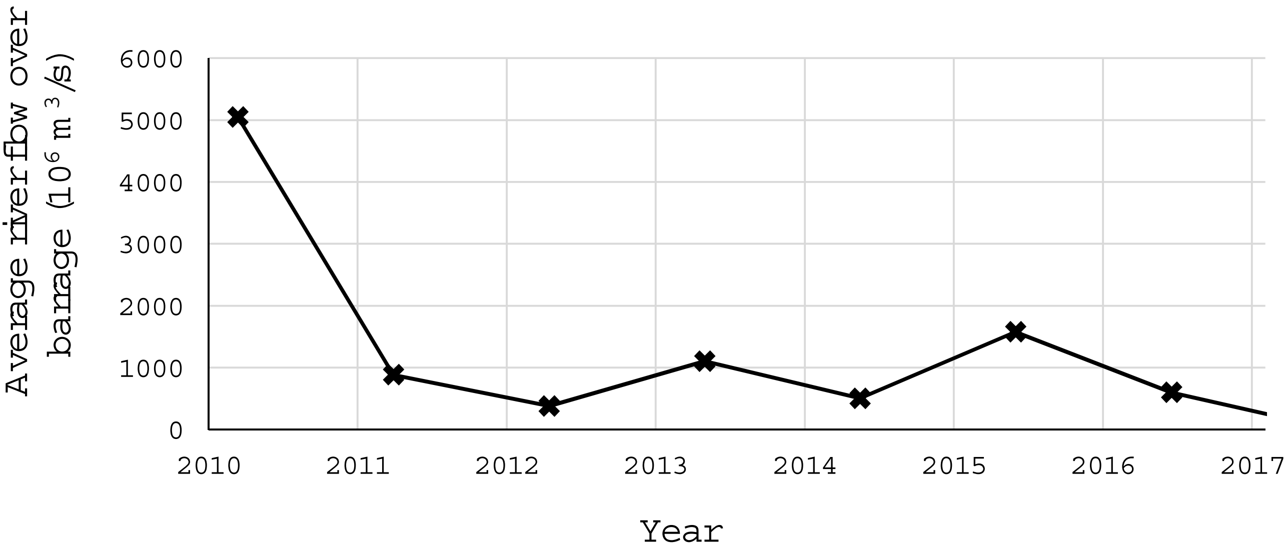

Average river flow over barrage (106 m3/s)
6000
5000
4000
3000
2000
1000
0
2010
2011
2012
2013
2014
2015
2016
2017
Year

(b)

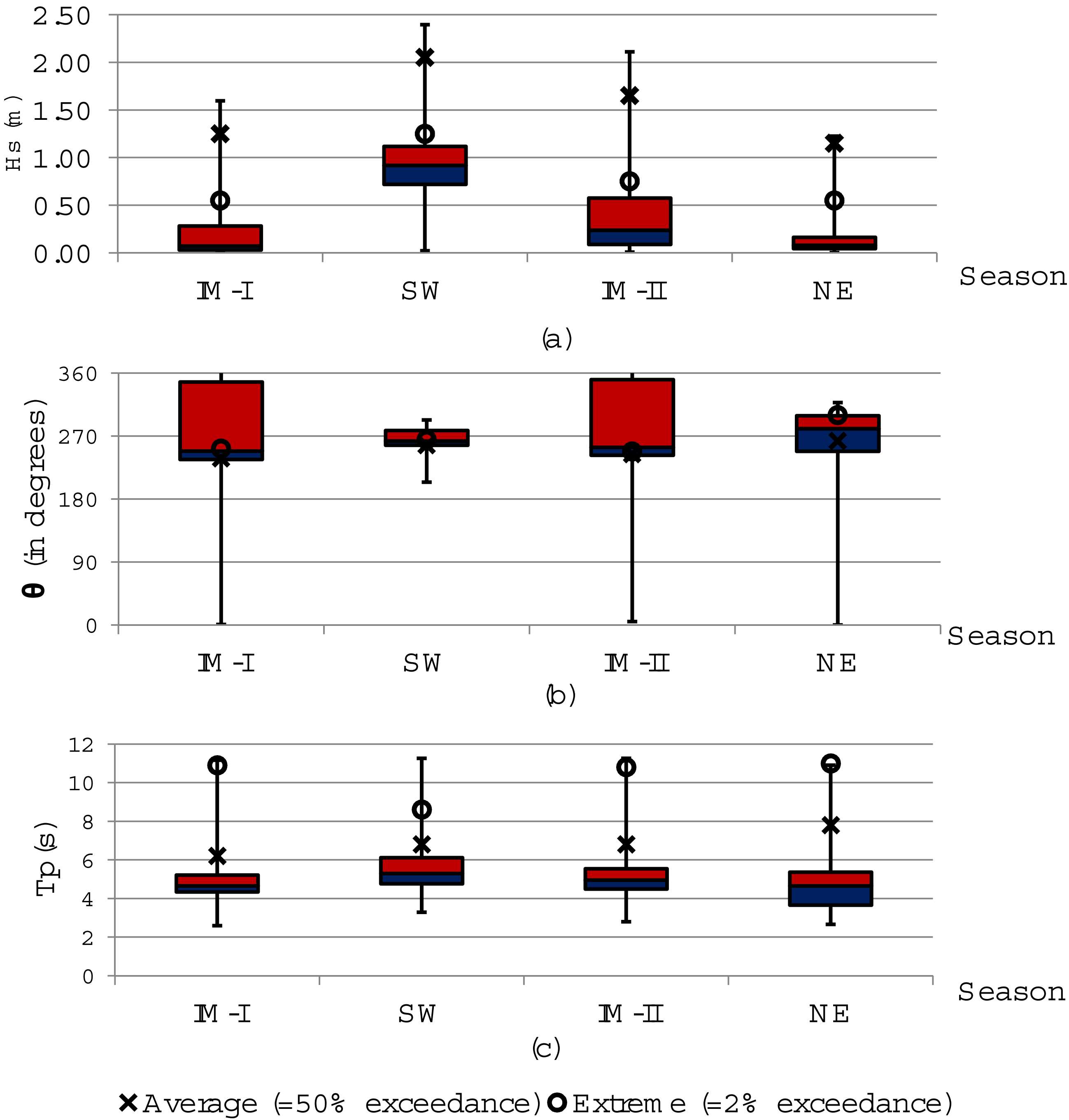

2.50
2.00
1.50
1.00
0.50
0.00
Hs (m)
Season
IM-I
SW
IM-II
NE
(a)
360
270
180
90
0
θ (in degrees)
Season
IM-I
SW
IM-II
NE
(b)
12
10
8
6
4
2
0
Tp (s)
Season
IM-I
SW
IM-II
NE
(c)
Average (=50% exceedance)
Extreme (=2% exceedance)

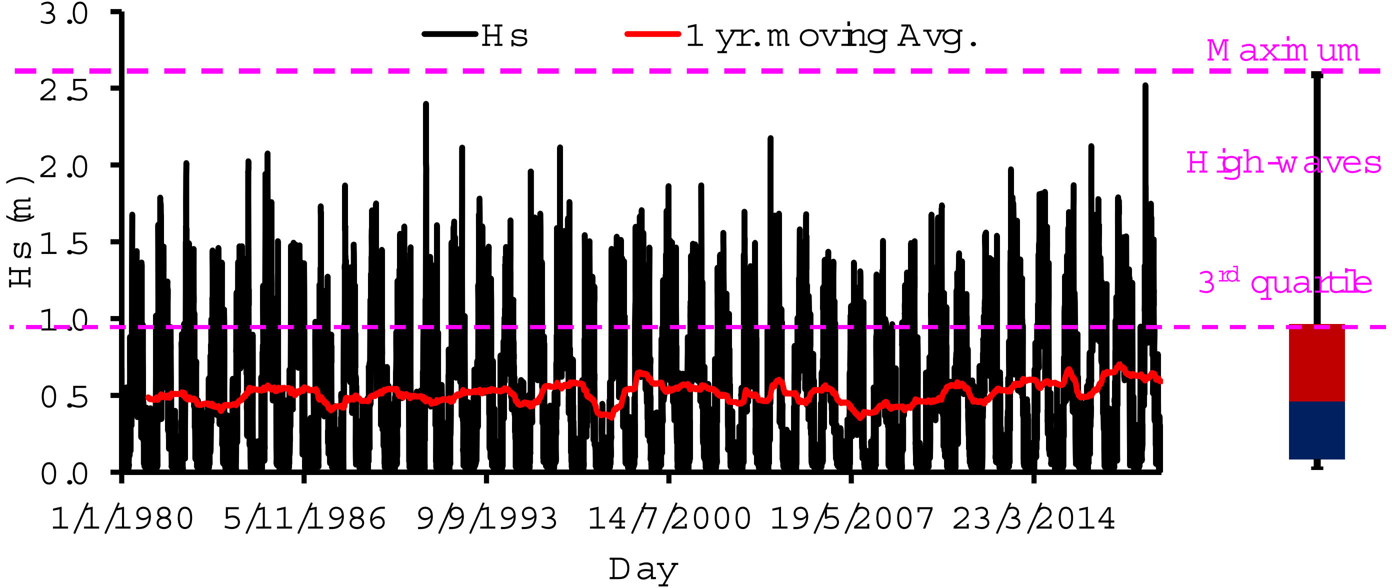

Hs
1 yr. moving Avg.
Maximum
High-waves
3rd quartile
Hs (m)
3.0
2.5
2.0
1.5
1.0
0.5
0.0
1/1/1980
5/11/1986
9/9/1993
14/7/2000
19/5/2007
23/3/2014
Day

(a)

(b)

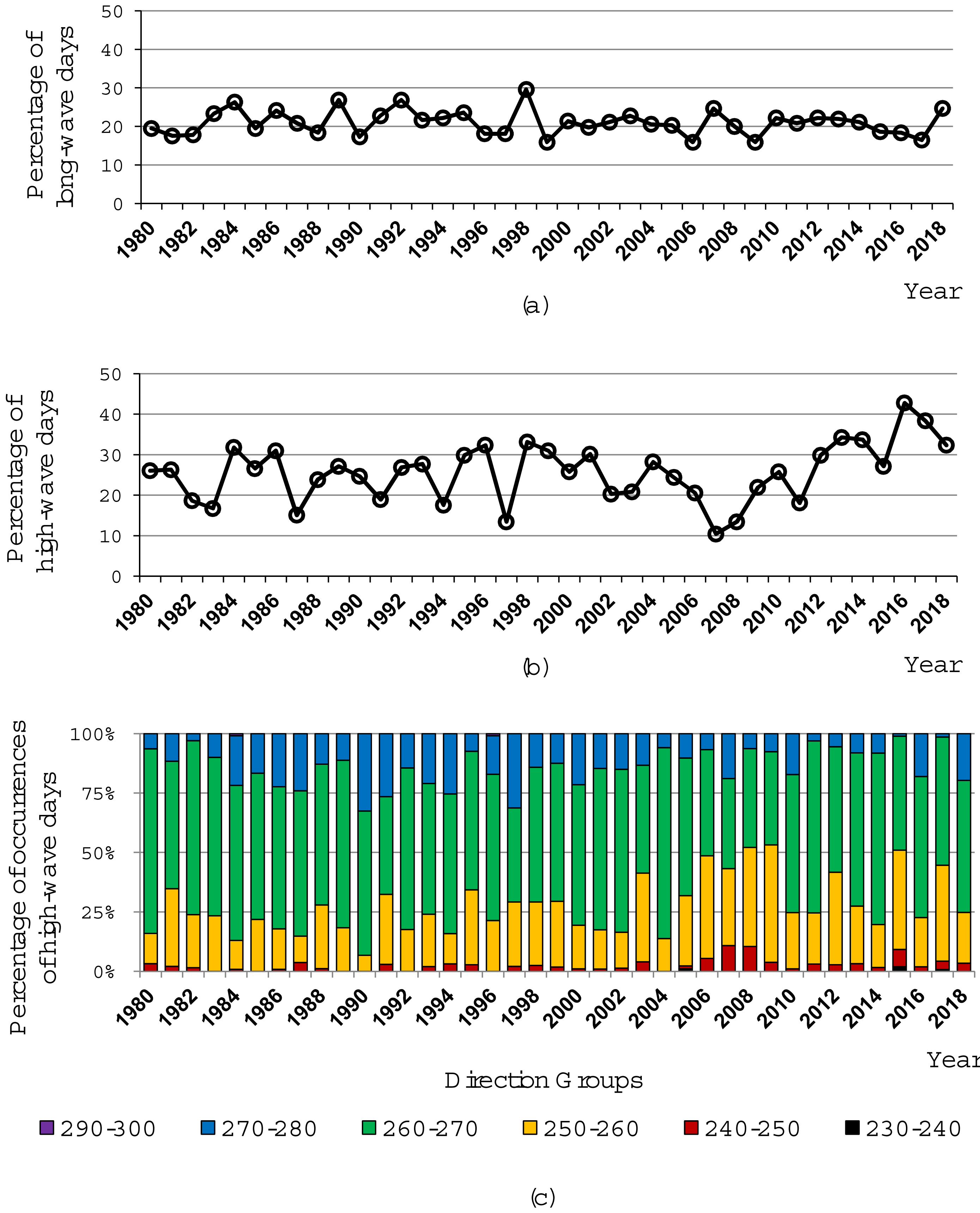

Percentage of long-wave days
Year
(a)
Percentage of high-wave days
Year
(b)
Percentage of occurrences of high-wave days
Year
Direction Groups
290-300
270-280
260-270
250-260
240-250
230-240
(c)

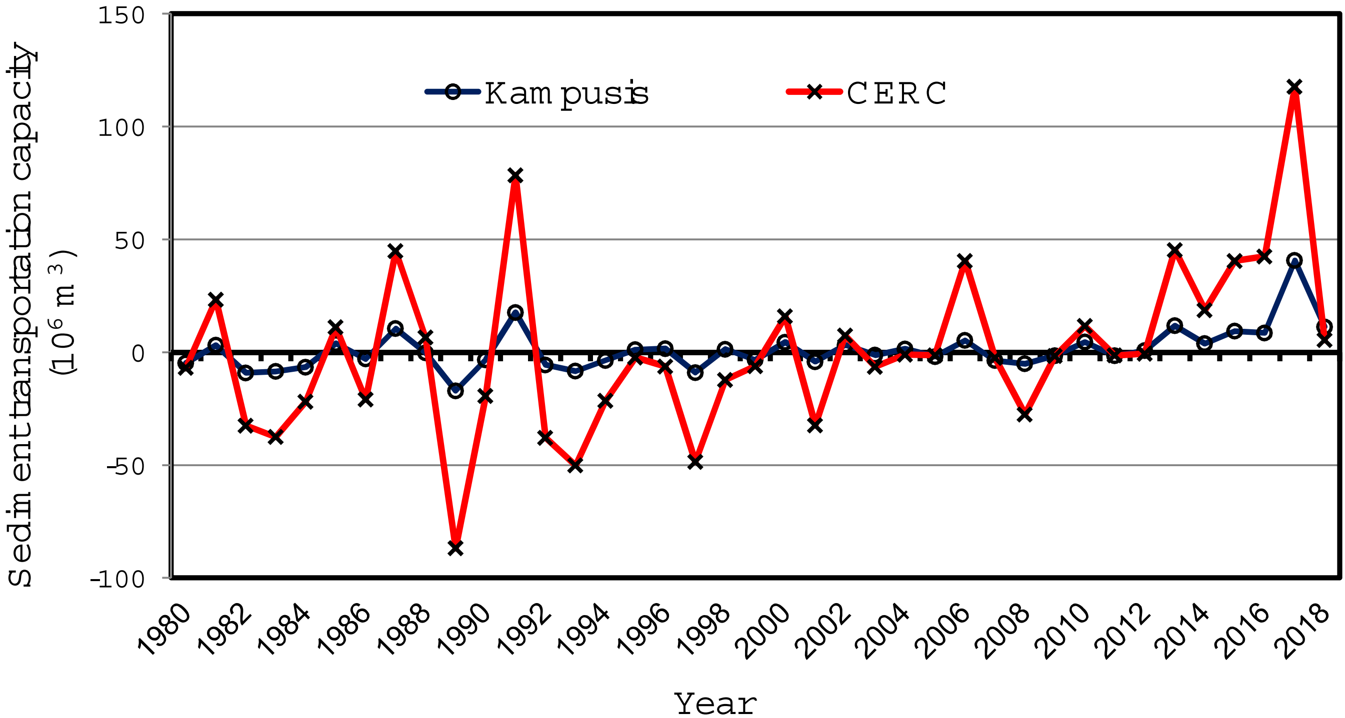
Sediment transportation capacity (10^6 m^3)
150
100
50
0
-50
-100
Kampusis
CERC
1980
1982
1984
1986
1988
1990
1992
1994
1996
1998
2000
2002
2004
2006
2008
2010
2012
2014
2016
2018
Year

(a)

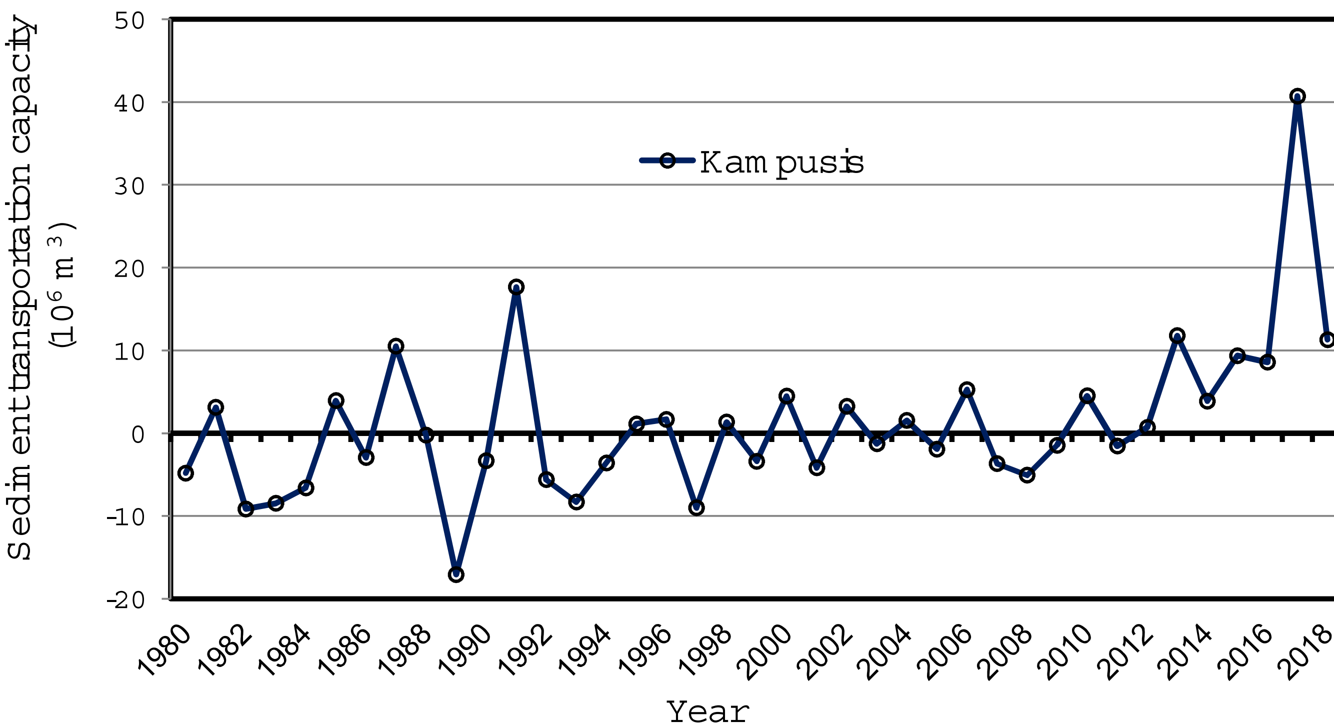
Sediment transportation capacity (10^6 m^3)
50
40
30
20
10
0
-10
-20
Kampusis
1980
1982
1984
1986
1988
1990
1992
1994
1996
1998
2000
2002
2004
2006
2008
2010
2012
2014
2016
2018
Year

(b)

(a) Feb./2017

(b) Aug./2017

(c) Feb./2018

(d) Feb./2019

(e) Feb./2017

(f) Aug./2017

(g) Feb./2018

(h) Feb./2019

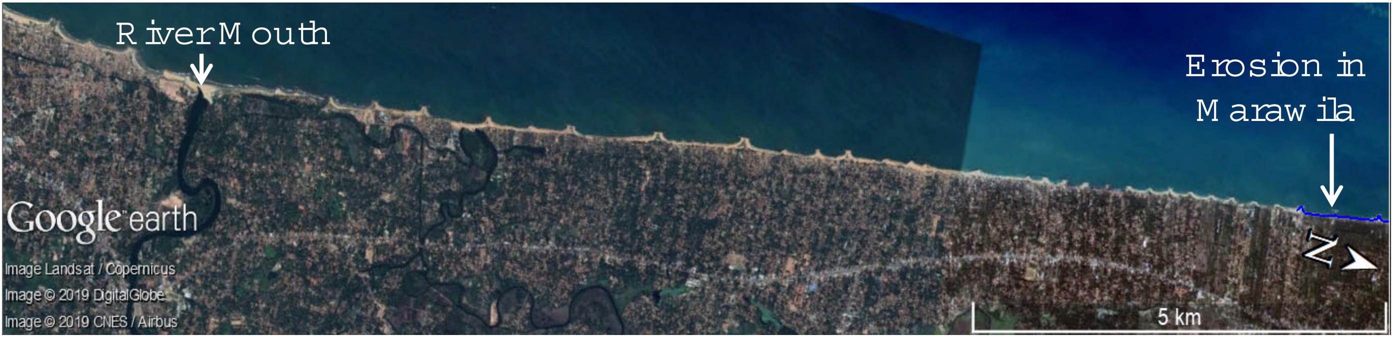
River Mouth
Erosion in
Marawila
Google earth
Image Landsat / Copernicus
Image © 2019 DigitalGlobe
Image © 2019 CNES / Airbus
5 km
N

(a)

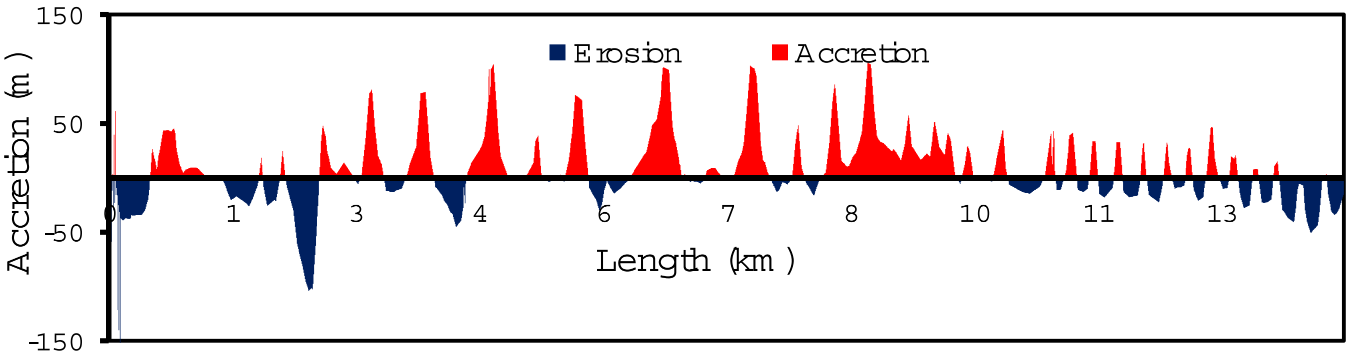
Erosion
Accretion
Accretion (m)
150
50
-50
-150
0
1
3
4
6
7
8
10
11
13
Length (km)

(b)

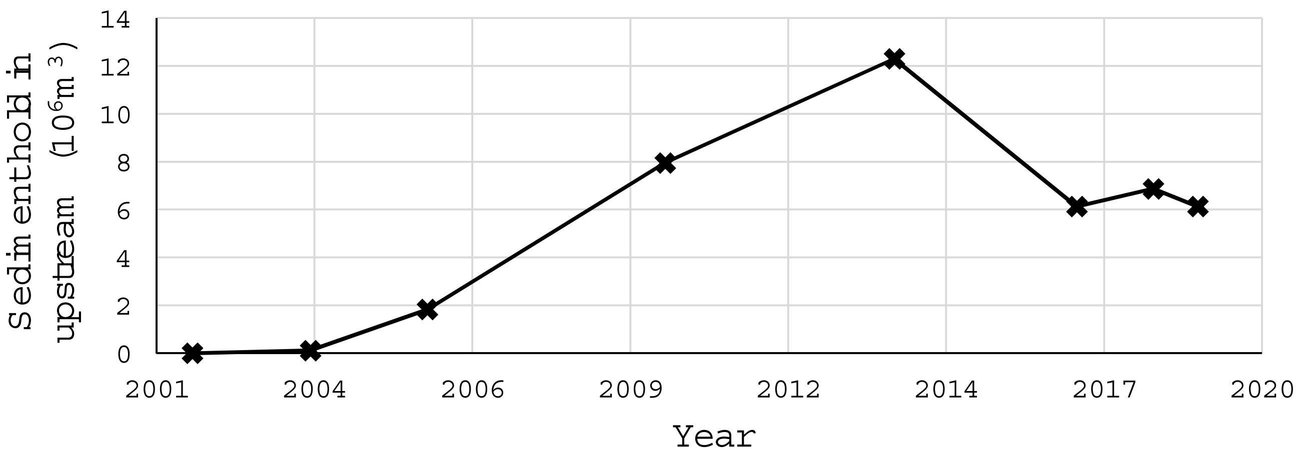
Sediment hold in upstream ($10^6 m^3$)
14
12
10
8
6
4
2
0
2001
2004
2006
2009
2012
2014
2017
2020
Year

(c)

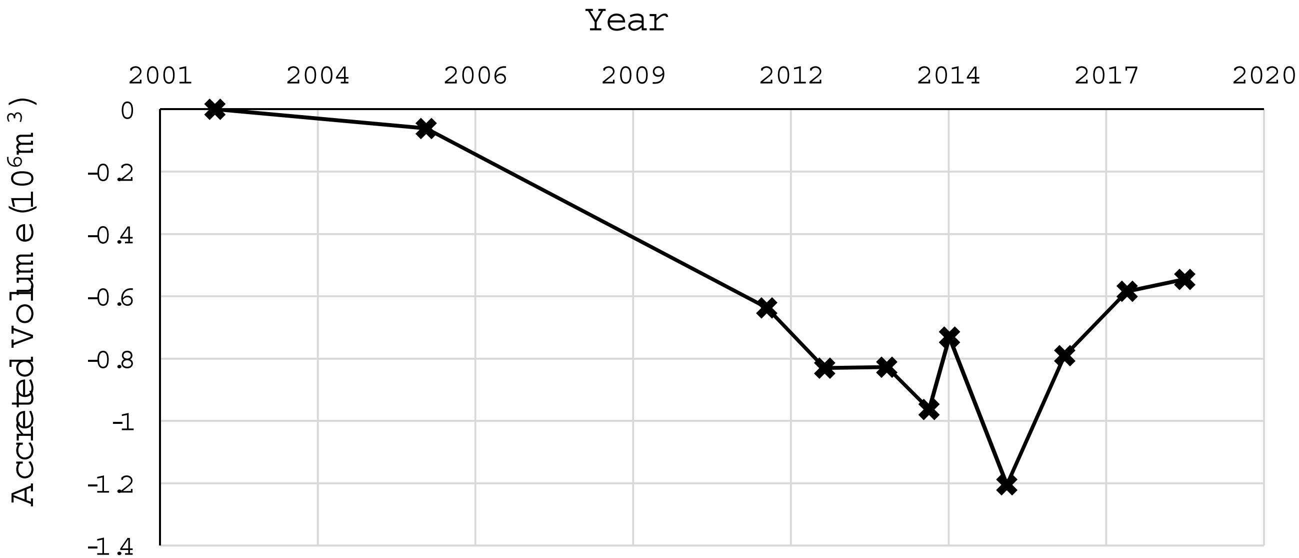

Year
2001
2004
2006
2009
2012
2014
2017
2020
0
-0.2
-0.4
-0.6
-0.8
-1
-1.2
-1.4
Accreted Volume ($10^6 m^3$)

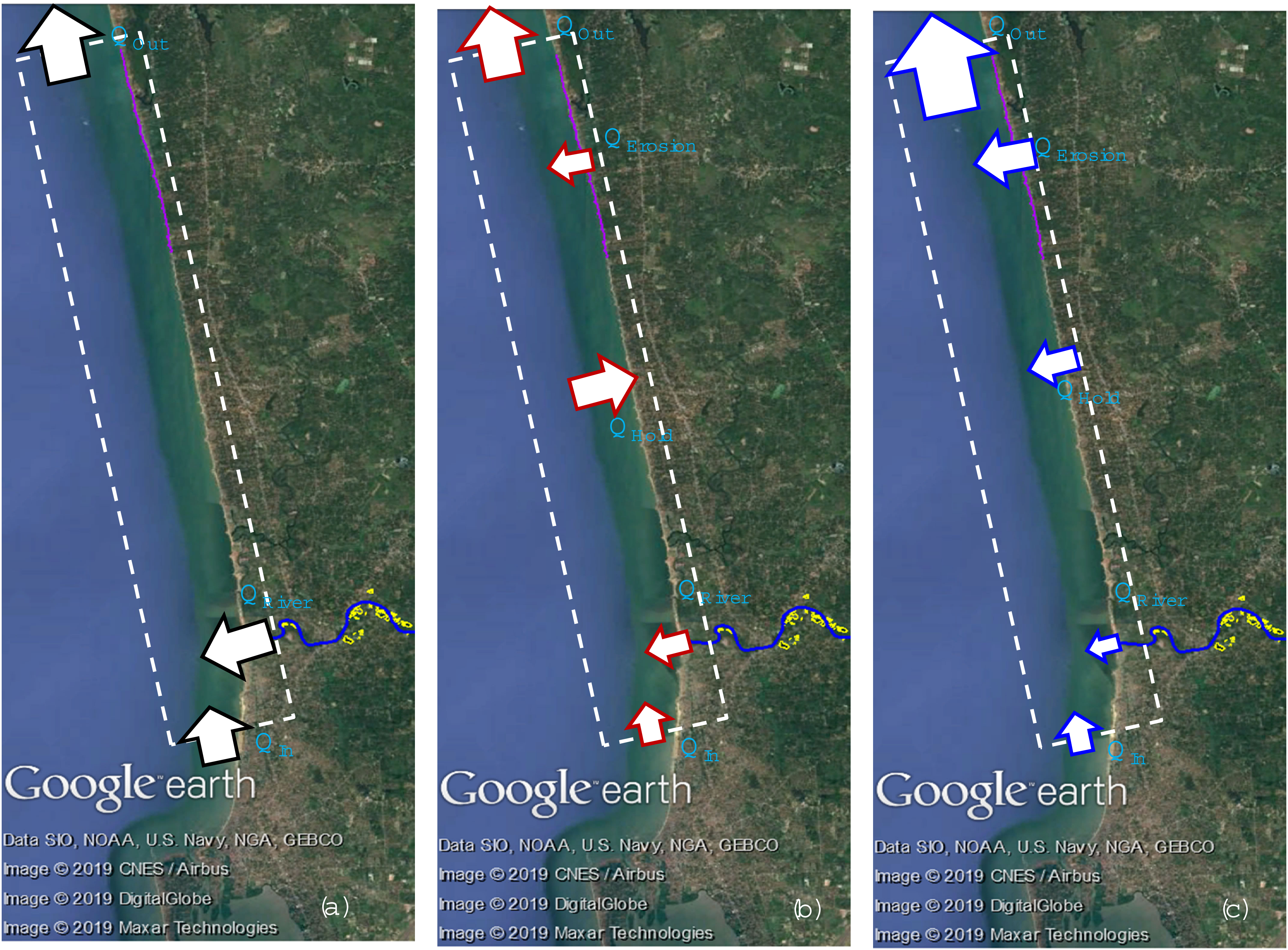
Q Out
Q Erosion
Q Hold
Q River
Q In
Google earth
Data SIO, NOAA, U.S. Navy, NGA, GEBCO
Image © 2019 CNES / Airbus
Image © 2019 DigitalGlobe
Image © 2019 Maxar Technologies
(a)
(b)
(c)